Ballistic Protection Panels Based on Glass Fibers Fabrics

George Ghiocel OJOC

GALATI UNIVERSITY PRESS
2024

Copyright © 2024 Galaţi University Press

Toate drepturile rezervate. Nicio parte a acestei publicaţii nu poate fi reprodusă în nicio formă, fără acordul scris al editurii.

Colecţia Ştiinţe Inginereşti

Galaţi University Press – Cod CNCSIS 281
Editura Universităţii „Dunărea de Jos”
Str. Domnească, nr. 47, 800008 – Galaţi, ROMÂNIA
Tel. 0336 130 139; Fax: 00 40 236 461 353
gup@ugal.ro

Referenţi Ştiinţifici:

Prof. univ. dr. ing. Lorena DELEANU

Conf. univ. dr. ing. Constantin GEORGESCU

ISBN 978-606-696-311-4

Publicate cu ajutorul Editurii Universităţii “Dunărea de Jos” din Galaţi - GALATI UNIVERSITY PRESS.

Preface

This is an extended abstract of a study dedicated to composites based on glass fibre fabrics with applications as ballistic protection materials. It was prepared by the author as a PhD thesis, but is a good example of an experimental and modelling study.

The study is developed logically, with a chapter dedicated to the literature dealing with similar topics, a chapter modelling the bullet impact process with the help of finite element method, another chapter for producing, at laboratory scale, composite panels made of quadriaxial fabrics in high-quality epoxy resin matrix, a commentary on the results obtained experimentally and investigations for identifying the failure processes of the panels. Conclusions are logically presented and they link model and experimental data through validation criteria. The book ends with a rich and recent bibliography on the ballistic impact behaviour of composites with glass fibres.

The results are of interest in the field of lightweight armour design and fabrication for vehicles and enclosures, both for those producing such systems and for researchers developing similar topics.

Professor eng. Lorena Deleanu, PhD

Acknowledgement

I would like to thank those who supported me and guided me through this doctoral thesis.

I would like to thank professor eng. Lorena Deleanu, PhD, who, as a scientific supervisor, offered me guidance, encouragement during the years of elaboration of the thesis.

Thanks also to the advisory commission, formed by professors physicist Gabriel Murariu, PhD, physicist Adrian Cîrciumaru, PhD and associate professor Constantin Georgescu, PhD.

I did the tests with the help of physicist Simona Sandu, PhD, and the staff from CCIACBRNE - Center for Research and Innovation for CBRN Defense and Ecology, Bucharest.

I would like to thank INAS Craiova SA, especially to Irina David and. Florian Vlădulescu, for their recommendations and technical assistance in using Ansys Explicit Dynamics.

I would like to thank eng. Cătălin Pîrvu, PhD, researcher at "Elie Carafoli" National Institute for Aerospace Research – INCAS, Bucharest, for the recommendations done for designing the model withthe help of finite element method.

For SEM images, obtained with the help of the scanning electron microscope from the "Dunărea de Jos" University, patiently searched, discussed, and well-argued investigation of the failure mechanisms, I thank physicist Alina Cantaragiu Cioromila, PhD.

For the support given in using the oven from "Dunărea de Jos" University, I thank the universitary lecturer. chemist engineer Dumitru Dima, PhD.

Thanks to those from MartPlast Urziceni, especially to Dan Iorga and Mihai Victor Popescu, with whom I collaborated for manufacturing the protection panels and with whom I participate to the invention salon at the "Nicolae Bălcescu" Land Forces Academy in Sibiu.

This doctoral thesis was supported by the project "Excelența academică și valori antreprenoriale - sistem de burse pentru asigurarea oportunităților de formare și dezvoltare a competențelor antreprenoriale ale doctoranzilor și postdoctoranzilor - ANTREPRENORDOC" ("Academic Excellence and Entrepreneurial Values - Scholarship System to ensure opportunities for training and development of entrepreneurial skills of PhD and postdoctoral students - ANTREPRENORDOC"), project code: SMIS 123847, contract code POCU/380/6/13.

With gratitude and love, I offer thanks to my parents and my sister, who have supported me during this time.

Eng. George Ghiocel Ojoc

Galați, 21.04.2022

Summary

Acknowledgement 3
Summary 5
Chapter 1. Analysis of the recent state of using fiberglass for impact protection system 7
1.1. Fibers used for ballistic protection systems 7
1.2. Fabrics for protective systems 9
1.2.1. Types of fabrics in composites for protection systems 9
1.2.2. Glass fibres 10
1.3. Design of a protection system 12
1.4. Issues related to testing and evaluation of glass fiber protection systems 15
1.5. Conclusions on the use of glass fibers for ballistic protection 17
1.6. Research directions for this study 17
Chapter 2. Organization of the thesis 18
Chapter 3. Model of the impact projectile - layered plate, at macro level 19
3.1. Material constitutive models 19
3.2. Failure criteria 20
3.3. The model for an impact projectile - ballistic stratified panel 21
3.3.1. The involved bodies and the model conditions 21
3.3.2 Mesh network 22
3.3.3 Material models of the bodies involved in the model 23
3.4. Results of simulation and discussions 26
3.4.1. The aim of simulations 26
3.4.2. The influence of impact velocity on the modeled pane 31
3.4.3. Simulation of a panel thickness range, for v_0 = 375 m/s … 35
3.5. Conclusions 38
Chapter 4. Laboratory-scale technology of ballistic protection panels 41
4.1. The involved materials 41
4.1.1. Glass fibers and glass fiber fabrics 41
4.1.2. Epoxy resin matrix 42
4.2. Laboratory-scale technology for obtaining the designed panels 44
4.3. Characterization of elaborated panels 48
4.4. Conclusions concerning the fabrication of the panels 49
Chapter 5. Experimental campaign and evaluation of results 51
5.1. Ballistic protection standardization 51
5.2. Test campaigns for rigid panels (shields or shield components) 54
5.3. Test equipment 55

5.4. Test methodology 55
5.5. Results obtained from the performed tests 56
5.6. Failure mechanisms in tested composites 61
5.7. Identification of the components that participated in the impact by EDX analysis 65
5.8. Conclusions on the ballistic impact behavior of the designed panels 68
Chapter 6. Conclusions and personal contributions 69
6.1. The importance of the theme 69
6.2. Final conclusions on the ballistic resistance of the tested panels 69
6.3. Personal contributions 75
6.4. Research directions open by this thesis 77
Author's scientific work 79
References 81

Chapter 1. Analysis of the Recent State of Using Glass Fibers for Impact Protection Systems

1.1. Fibers Used for Ballistic Protection Systems

The field of high-performance fibers has been of great economic interest [38] for only 100 years, but offers innovative technologies, relevant to impact protection systems [12], [24], [30].

In 1960, DuPont developed polyparaphenylene terephthalamide, a much more rigid linear molecule that resulted in the spinning of a crystalline liquid solution, obtaing fibers with a high degree of crystallinity. Today, these and similar fibers, such as Twaron [72], are essential in the fabrication of personal protective equipment. Other polymeric fibers are particularly designed for ballistic protection, such as: very high density polyethylene (UHMWPE), polybenzobizoxal (PBO), polybenzenimidazole (PBI) [7], [14].

Graphs for several mechanical characteristics, for different fibers, involved in impact resistance, are given in Fig. 1.1; for nylon the strain at break values are not given here because they are between 1.5-2.5, much higher than the values of the other fibers in the graph.

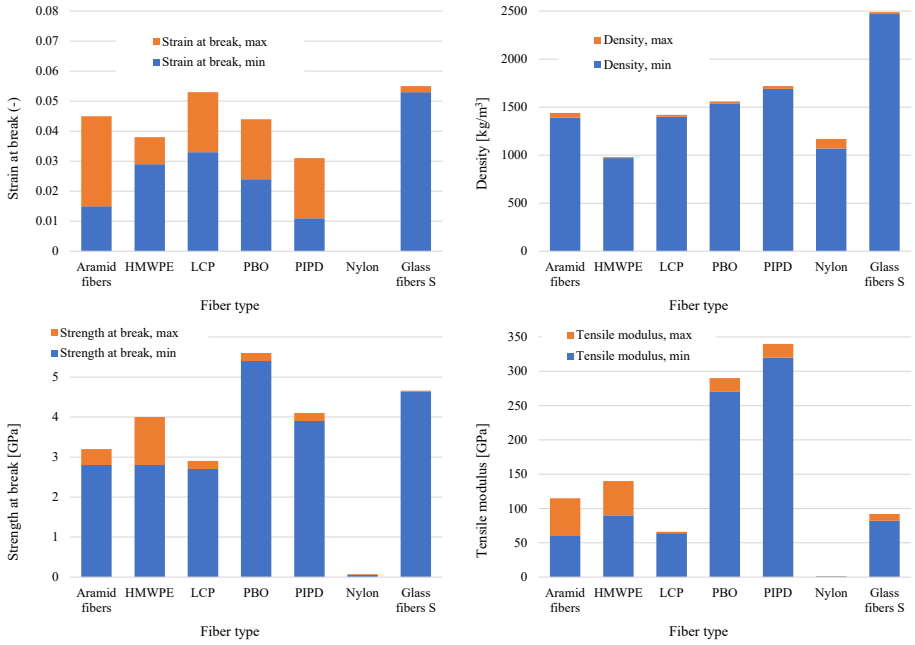


Fig. 1.1. Mechanical characteristics, involved in impact resistance, for fibers (HMWPE - very high density polyethylene, LPC - liquid crystal polymers, PBO - polybenzoxazole, nylon - polyamide fibers, PIPD - polybenzimidazole) [28]

Although glass fibers have some disadvantages, they are currently used to protect vehicles and other systems that ask for impact protection. The development of a glass fiber protection system involves several aspects:

- the quality of the fabrics, but also of the fibers and yarns,
- the quality of the matrix (the resin or polymer that will "bind" the yarns and layers together),
- the effectiveness of the technology in achieving fast, repeatable, with the same degree of quality, systems of different sizes and shapes, required for a certain application, relatively lower costs, but higher specific densities,
- availability and interchangeability, usage time and even recycling.

Tensile strength of fibers increases with decreasing fiber diameter and is limited by fiber defects, residual stresses and structural inhomogeneities. The risk of finding defects decreases with decreasing fiber diameter. Nowadays, carbon fibers have diameters between 4 μm and 10 μm; for polymeric fibers and most ceramic and glass fibers, the diameters are in the range of 10 μm to 15 μm [45].

Ballistic impact behavior of polymeric, metallic or ceramic fibers is characterized by their ability to locally absorb the kinetic energy of the projectile and to transmit the absorbed energy rapidly along them, before characteristic condition(s) of failure, quantified by absorbed energy per mass unit, E_{sp}, are met, that is related to the strength limit, σ_{fail}, the fiber strain at break, ε_{fail}, and the fiber density, ρ, and $E_{sp} = 0.5\sigma_{fail}\ \varepsilon_{fail}/\rho$. The ability of fibers to dissipate energy is governed by the speed of sound through the material, the modulus of longitudinal elasticity, E, and their density, ρ, in the form $v_{sound} = (E/\rho)^{(1/2)}$. Glass fibers have a good positioning of the absorbed energy per mass unit as compared to some polymer fibers [9], [28].

1.2. Fabrics for Protective Systems

1.2.1. Types of Fabrics in Composites for Protection Systems

A major criterion for impact-resistant structures, which also include glass fibers, is the architecture of yarns. Studies on protection systems with layered or hybrid composites are done at different levels: from micro level for fibers and yarns, to meso level dealing with fabrics and layers, to macro level, when simulation and experimental results are given for the whole protective structure. The recent performances of computers (hardware and software) make possible simulations of ballistic processes, taking into account the yarns and several layers of yarns [51].

The properties of long fiber reinforced composites depend on their nature, the yarn architecture, the matrix and assembly technology, the fraction volume of fibers, thickness of the package. Glass fibers have a high resistance to relatively low costs; carbon fibers have higher strength, high rigidity and lower density, aramid fibers have high strength and low density, preventing the fire spread and are penetrated by radio waves. Polyesters are often used as a matrix because they provide good properties at relatively low cost. Epoxy resins and polyamides have better properties, but are more expensive. The strength of composites increases if the volume fraction of the fibers is higher and if the orientation of the fibers is parallel to the load direction [3], [20], [31].

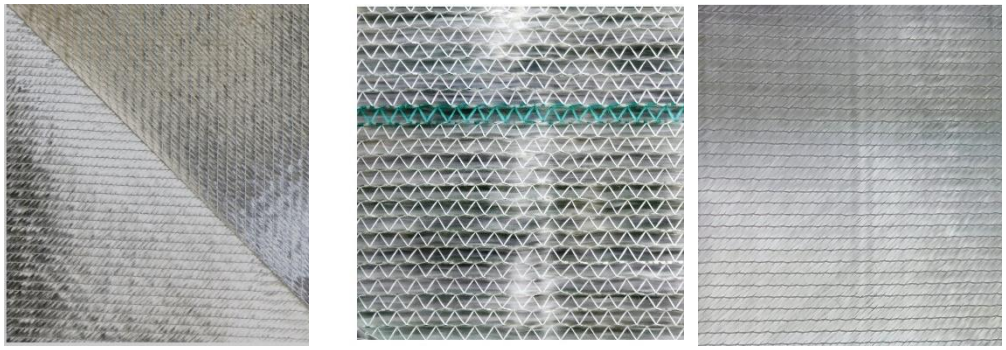
According to the architecture of fibers and yarns, fabrics may be classified into woven, knitted and non-woven or unidirectional materials. In the latter, the yarns are not crimped, being able to keep all their resistance to overcome the stress resulting from the impact [45]. Fabrics can also be classified according to many criteria, including water retention, fire resistance, ballistic protection etc. Traditionally, a composite dedicated to ballistic protection is based on a 2D architecture.

The 2D architecture includes unidirectional yarn arrangements, with variants, such as (0°/90°), (0°/90°/45°), (0°/90°/45°/-45°), and the woven ones are 1/1(plain), basket type, satin, twill etc. Attachment of fiber layers is a matter of material(s) and technology (laying-up, vacuum or pressure forming, sewing etc.). Consequently, the composites are controlled in thickness by the weaker constituent, usually the matrix, and in terms of the properties of yarns and fibers.

Castro company has in its portfolio pre-pegs products based on glass fibers, unidirectional (Fig. 1.2), woven or mat/woven combinations. They have flexibility, but also mechanical strength and are suitable for impact-resistant components. The recommended resins for composite are polyesters, vinyl esters and acrylic-urethane resins.

The advantages of unidirectional fabrics (single or multiaxial) include better specific mass and strength of the fibers to support the external load and not the bending introduced by the technological process (as in weaving), fiber orientations can be at 0°, 45°, 90°, even -22.5° and +22.5°, drapery and permeability (if needed), could be taylored.

In general, multi-axial semi-finished products reduce cost and processing time for the final product [79].



a) Unidirectional biaxial fabric, (+45°/-45°), 800 g/m^2

b) Unidirectional fabric, with auxiliary knitted yarns, 1200 g/m^2

c) Quadriaxial stiched fabric (0º/+45º/90º/-45º), 1200 g/m^2

Fig. 1.2. Fabrics produced by Castro Company [79]

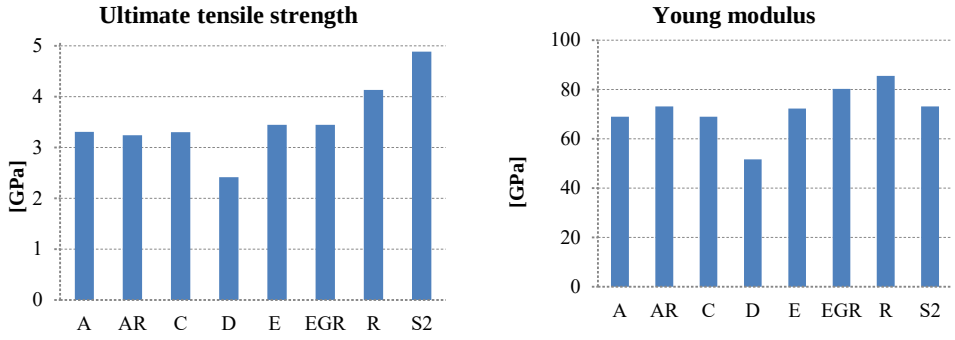
1.2.2. Glass Fibers

Glass filaments or fibers are versatile materials, produced by melting silicon oxide and other minerals, with rapid cooling to prevent crystallization and fibrillation [67]. The types of glass fibers have been grouped according to one of the characteristics for which they are used: E, S, C, A and D [42], [64].

Glass fibers and glass fiber fabrics have a wide range of applications, from mechanical, electrical, corrosion protection ones to narrow applications, such as ballistic protection. Among the groups of glass fibers, types E and S (including variant S2) are fibers with better mechanical

performance. Type E is composed of CaO, Al_2O_3 and SiO_2, sometimes with B_2O_3, from 0 to 10 wt.%. These fibers are suitable for fabricating, by different techniques, composites with glass fibers (found in the literature with the abbreviation GFRP - glass fiber reinforced polymer) [45]. In general, type S2 has a resistance 35% to 40% higher than type E [45] and has a better performance in ballistic protection, for composite or laminated shields. The rather high tensile strain, as compared to other ballistic protection materials, plays an important role in the ballistic impact mechanism. Glass fiber structures are also recommended for fire, smoke and toxic gases protection, they have relatively lower cost and lower specific mass as compared to metal alloys or reinforced concrete. The advantages of glass fibers are: relatively low price, tensile and impact resistance, chemical resistance, but they also have disadvantages, such as low modulus of elasticity, abrasion wear, low fatigue strength and poor adhesion to some resins, which raises the price by selecting a relatively expensive matrix [1].

Figure 1.3 provides mechanical and thermal properties for different types of glass fibers and it is observed that type E (with or without boron) has good mechanical properties, being surpassed only by type S.



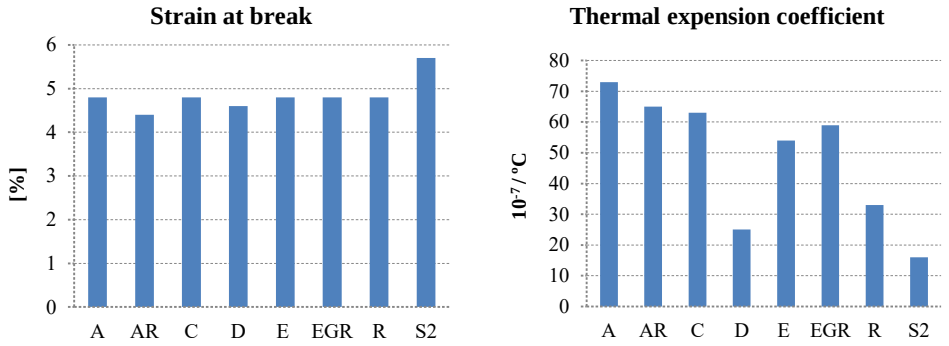


Fig 1.3. Characteristics of glass fiber (after [60])

A - glass with durability, mechanical strength and electrical resistivity, C - glass with corrosion resistance, D - glass with low electrical constant, E - glass with high mechanical strength and electrical resistivity, AR - glass with alkali corrosion resistance, R - glass with mechanical and acid corrosion resistance, EGR - glass for exhaust gas recirculation systems, S - glass with the highest tensile strength, S2 - glass with high tensile strength, high modulus of elasticity and stability

In the field of ballistic protection, the most commonly used types of fabrics are 1/1 and basket-type fabrics. Fabrics are also produced with unidirectional yarns, with one or more orientations (two, three and four), for the latter type, the angle between the yarns of the sub-layers varying from (0°/90°), (-45°/45°) up to (0°/90°/-45°/45°). Cunniff observed that loosely woven or unbalanced weaving leads to poor ballistic performance [21].

In general, fibers with a relatively higher strain at a high strain rate, absorb energy better than those with a relatively low strain at break [10], [49]. The fiber-matrix interface plays a critical role in impact resistance. It has been observed that poor interfacial interaction has led to higher energy absorption [2], [54], [63], but each matrix must pass the experimental test to be accepted. Composites made of fabrics have particular failure mechanisms, such as fibers' break, fiber-matrix detachment, delamination, sliding, matrix cracking, but also friction between components and between them and projectiles promotes the energy absorption.

1.3. Design of a Protection System

Figure 1.4 presents a logic diagram for the design of a new protection system, highlighting a tighter loop of research for the development of new

materials, modeling and simulation, resulting in a significant reduction in time for developing a new armor. Issues related to the restriction of information in the field lead to the development of only punctual or partially effective solutions [69]. The feedback loop between the design of the protection system and the design of the material is in contrast to current practice, in which the design flow puts the new materials "on the shelf" to be tested in the testing process.

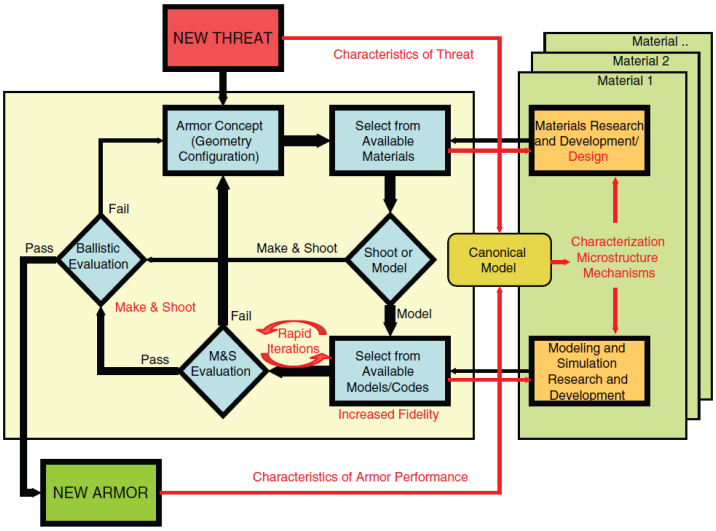


Fig. 1.4. Logic diagram for re-designing body or equipment armor [69]

The performance parameters of a composite shield include measurable, but also qualitative parameters [25]. The most important measurable parameter is the ballistic limit, i.e. the velocity at which a certain projectile can pierce a certain target. It is also important to respond to multiple hits and tolerances of target material and geometric characteristics, especially to partial penetrations, when damage to the target face and back is concerned, to assess the long-term survival of the protected system [39]. Other parameters include surface density, machinability, interchangeability, maintenance and costs of replacing the old solution etc. [68].

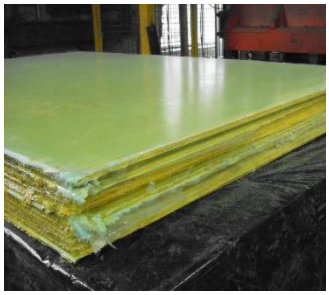
The first composite shield was made in the mid-1950s by American specialists, under the name T95, and consists of a layer of silicates arranged between two steel plates, the assembly being made by rolling [15].

Composite shielding has the following advantages: good impact resistance, good vibration damping capacity, relatively low power consumption for small or high series technology, good resistance to corrosive agents, if the components also have it (resin and fibers), good resistance to high temperatures, specific masses 2-3 times smaller than steel. Composite shields are also used in vehicles for transporting personnel or equipment, being most often inserted in the vehicle body, between metallic surfaces.

Protectolite Composites [73] produces ballistic protection plates (sheets) made of glass fiber, obtained by compression in the mold, with high precision and repeatability. They are manufactured in sizes from 600 mm x 600 mm to 1525 mm x 4000 mm. Laminated boards can be made of aramid, carbon, but also glass fiber fabrics, type E or S, using as matrix or adhesive thermosetting resins (vinylester, phenolic or epoxy) and thermoplastic foils or resins. The produced panels can be used for military vehicles, secure vehicles and buildings, personnel security vehicles, armored vehicles for transporting valuables, composite armor for other purposes and aerospace platforms or applications thereon (housings for cameras or measuring devices). The plates also provide protection against severe threats to jeeps, military supply trucks. They are also used for police equipment and architectural solutions that require a high degree of protection, including in court (Fig. 1.5).



a) armored vehicle



b) component of the armor, made as composite



c) armored components based on glass fibers panels for military vehicles

Fig. 1.5. Products of the company Protectolite Composites [73]

1.4. Issues Related to Testing and Evaluation of Glass Fiber Protection Systems

In Figure 1.6, the panel made of glass fibers and epoxy resin stopped the bullet, the mass ratio of fibers to the height of the plate cross section being about 70%, the manufacturing parameters of the panel being quite severe [22].



Fig. 1.6. Composite with glass fiber and resin, 13 mm thick, after impact with 9 mm FMJ projectile, at a speed of 420 m/s [22]

Ansari and Chakrabarti [8] presented an experimental and numerical analysis of the perforation behavior of laminated composites, reinforced with unidirectional glass fibers, after impact with a cylindrical projectile, with a flat impact surface, for impact velocities between 50-500 m/s. Different direction impact tests were performed using a pneumatic rifle. In general, delamination is the main damage to the plate hit by the projectile, when it hits the target normally, the magnitude of this damage decreasing as the angle of impact increases.

Rebouillat and others [57] compared three reinforcing materials (steel yarns, glass fiber and aramid fiber), analyzing the results of a composite cutting test. Composites have a synergic behavior as compared to their components, which is useful in impact protection applications. Research has been done on hybrid materials, using reinforcements with two or more fibrous components. The reinforcement arrangement is important, but the tests have been diversified (standardized or not) in order to reproduce as

plausibly as possible the actual load, for which the designed structure is used. Combinations of fibrous materials may give rise to better solutions for impact protection. For example, the brittle nature of glass fibers is restrictive for its shear strength, but it has a fairly good abrasive resistance. A more technologically resilient glass fiber or a more flexible fabric, obtained through the yarns' architecture and the technology of obtaining the pre-peg product, may be solutions to improve the response of glass fiber-based materials.

Sabet et al. [58] investigated glass fiber composites, reinforced with polyester resin, at an impact velocity of 80...160 m/s. Five types of E-type glass fibers were used, including short pressed fibers, 1/1 fabric, satin fabric, unidirectional fabric and bidirectional fabric (0°/90°). The projectile was a conical-head body, with a pointed tip at 30°, with a length of 15 mm, weighing 9.74 g. The composite plates (150 mm x 150 mm) were made with 3 mm and 6 mm thickness. The results showed a higher ballistic velocity limit for 3 mm chopped glassfiber boards, followed by bidirectional fabric, satin fabric, 1/1 fabric. Thicker specimens (6 mm) with 1/1 fabric showed better ballistic performance, followed by bidirectional fabric, satin fabric, unidirectional fabric and plates made of glassfiber, chopped and pressed. The dominant modes of failure were: yarn stretching and fiber breaking at shear for thinner plates, and severe delamination for thicker plates. Plates with 1/1 fabric and bidirectional fabric had a higher ballistic speed limit as compared to other types of reinforcements. The energy absorption associated with 1/1 fabric and bidirectional fabric had higher values.

The differences between simulation data and experimental data can be qualitatively explained by energy dissipation by friction between layers, as highlighted in [34].

In Romania, although there are working on local shielding solutions, the last significant appearance was a ProtectComb composite shielding study, in 2010 [75]. This shield contained, alternatively, layers of glass fiber and alumina ceramic composite in aluminum plate sandwich, replaced after ballistic evaluations with steel plates.

1.5. Conclusions on the Use of Glass Fibers for Ballistic Protection

In designing and testing solutions for ballistic protection, the novelties in the field of protection materials are taken into account, but also the areas not yet explored, so as to prioritize for testing materials and systems with better capabilities.

Although glass fiber composites compete with polymer fibers, metal or ceramic fibers, they are still of interest in ballistic applications, either as part of a shield or as a whole protection system, due to their good impact resistance at reasonable price. The research will be carried out in order to increase the ratio of fibers in the composite, but also to establish appropriate matrices for the application.

1.6. Research Directions for This Study

The impact of composites is and will be a challenge for researchers, given the increasing use of these materials and the wide variety of combinations that may be obtained based on existing matrices and reinforcing components. The challenge is to make a composite for protection so that its characteristics, as ballistic performance, structure and production technology, are competitive on the market, including highly complex products that are combinations of materials and technologies, some considered "classic", others of the latest.

The aim of this study is to design a composite based on unidirectional glass fiber fabrics, for a FB2 level shield or higher, for motor vehicles. The study will include a documentation, a proposal of laboratory-scale technology of the composites, simulations and experimental tests, investigations of the failure mechanisms and conclusions.

Chapter 2. Organization of the Thesis

Figure 2.1 shows a suggestive diagram for the organization of the thesis, which points out its objectives, the technology of producing the panels, simulation of their behavior in impact and testing and interpreting the results.

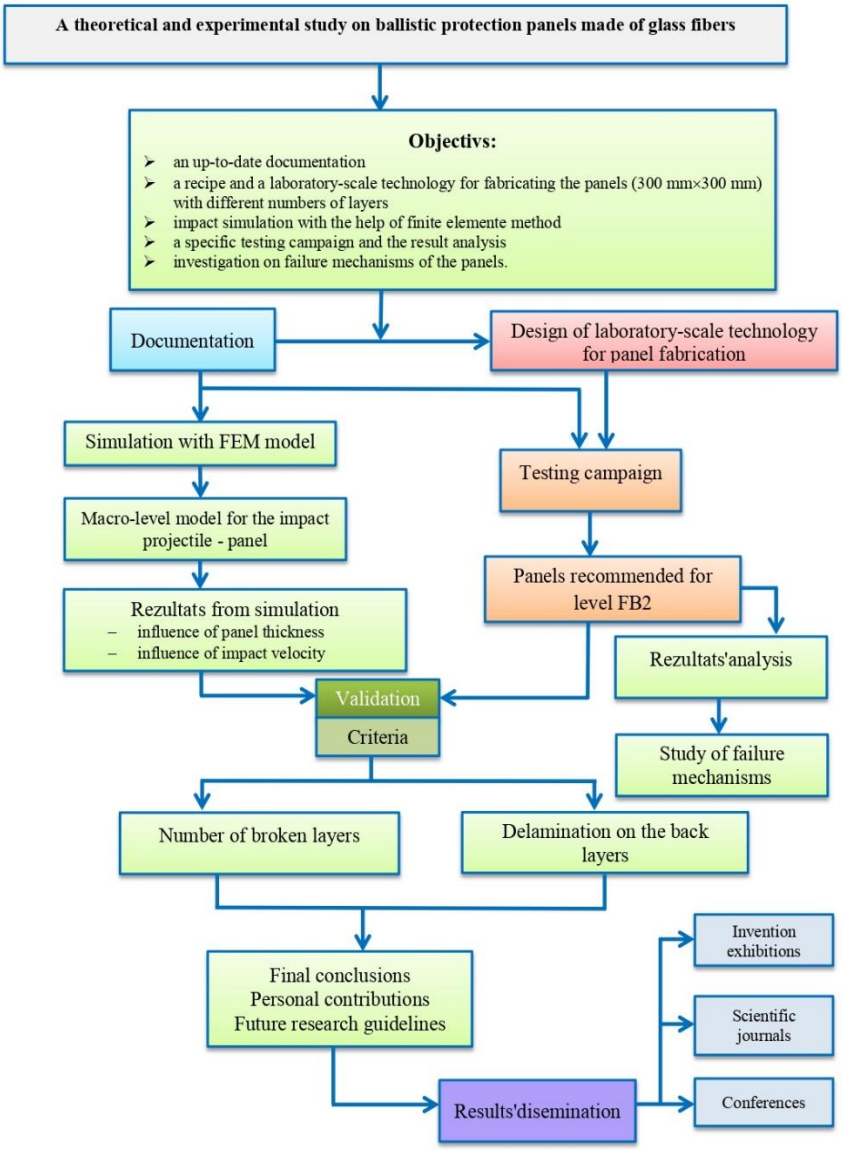


Fig. 2.1. Thesis diagram

Chapter 3. Model of the Impact Projectile - Layered Plate, at Macro Level

3.1. Material Constitutive Models

Materials, especially those used in impact processes, including ballistics, are characterized by a complex response (with many influencing factors) to impact or dynamic loading and these characterizations are the constitutive models of the materials. Among these aspects are: non-linear behaviour under stress, hardening or softening under stress variation and stress as a function of strain rate, softening under variable or steady temperature, compaction (for porous materials), orthotropic response (for composites, especially with long fibres), damage by crushing (for brittle materials as ceramics, glass, concrete etc.), processes characterized by chemical energy (blasts), particular failures or damages, phase changes (transitions from solid-liquid, liquid-gas or even solid-gas and vice versa). Three relationships are requested, the material strength model and the failure model, for modeling a material behaviour under load (steady, variable or under impact) and the state equation [23], [32], [40], [47].

In the case of impact projectile – target (a protection panel, for instance), constitutive models of the materials could be functions without temperature dependence, as this aspect is justified by films done with thermovision cameras, and by the results of simulations from the dedicated literature [6], [27], [28], [29], [43], [48], [52], [62]. Also, materials for fabrication of panels resisting to ballistic impact (such as aramid or glass fibre composites), have almost constant thermal characteristics over a large temperature interval. From the analyzed literature in the field, the modeling of an impact using a bullet (7.62 or 9 mm) in the range of impact velocity of 100-400 m/s is, thus, simulated under isothermal conditions. Of course, a thermal effect exists, but this is considered weak on the failure mechanisms of the solids involved in this impact (breaking, deformation, delamination, friction).

For layered or stratified composites, the adherence between two consecutive layers can be modelled with the help of the cohesive zone model with zero thickness (abbreviated CZM in literature), introduced for quantifying the interlaminar stress and layers' detachment (delamination), such as in [17], [36].

The bilinear hardening model is usually used, based on experimental data, in analyzes with large strains (especially for deformable bodies, not for brittle ones).

The Johnson-Cook model, introduced in 1983 and 1985 [35], [61] is generally used for metallic alloys, with high strain rates under load dynamics and high temperatures. The temperature dependence of stress-strain curves is not directly introduced. It shows the behavior of typical metallic materials, subject to high strains, strain rates and temperatures. In this model, the yield strength, Y, depends on strain, strain rate and temperature:

$$Y = \left[A + B\varepsilon_p^n\right]\left[1 + C\varepsilon_p^*\right]\left[1 - T_H^m\right] \tag{3.1}$$

where ε_p is the actual plastic strain, $\boldsymbol{\varepsilon_p^*}$ is the actual plastic strain rate, T_H is the relative temperature, as introduced in Johnson-Cook constitutive model (3.1), T_{room} is ambiental temperature, T_{melt} is the temperature at which the materials melts; this material model needs material constants (A, B, C, n and m), their values being experimentally determined.

3.2. Failure Criteria

The material library of Ansys [71] offers constitutive material models and for failure initiation, but it also offers the possibility of creating the user's model based on several equation. Any failure model has two components: crack initiation and post-failure response of the material.

There are several mechanisms for cracking in this software: failure achieved at critical plastic strain (often abbreviated to EPS), failure reached at a value for the principal stress, failure reached at principal strain, failure at tensile limit, failure according to Johnson-Cook model, exfoliation. When a specified criterion is met for an item, a post-failure response is set off.

The following failure models can be introduced in Ansys Explicit Dynamics: failure due to a critical value of plastic strain, failure at reaching a particular value for the principal stress, failure caused by a critical value of the principal strain, statistical failure, tensile failure, crack and relaxation failure, Johnson-Cook failure (meaning a cumulative failure produced by strain, strain rate and temperature) and failure by exfoliation.

Failure caused by a particular value of plastic strain (this being characteristic for a certain material and even load conditions) is characteristic for deformable materials. The initiation of failure is based on the actual plastic strain locally determined in the material. The user must enter a value of the maximum plastic strain. If the actual plastic strain of the material is greater

than this value, failure occurs. The material fails (it usually breaks) instantly. This failure model must be used in conjunction with a constitutive material model for stress evolution under load, either plastic or brittle.

The Johnson-Cook failure or damage criterion is recommended for constitutive models of ductile materials subjected to high pressures, large strain rates and high and/or large temperature intervals. The model for the material failure is introduced in a way resembling to Johnson-Cook constitutive material model. This failure model is described by 3 independent components that defines the failure by a value of dynamic strain till break as a function of temperature, stress and strain rate:

$$D = \sum \frac{\Delta_\varepsilon}{\varepsilon^f} \tag{3.2}$$

$$\varepsilon^f = \left[D_1 + D_2 e^{D_3 \sigma^*}[1 + D_4 \ln|\dot{\varepsilon}^*|]\right][1 + D_5 T^*] \tag{3.3}$$

ε^f is the plastic strain at break for the involved material, in particular conditions of loading, the first term is failure dependence on stress, using the constants D_1, D_2, D_3 (experimentally determined); the second term, D_4, shows how the strain rate influences the material failure, and the last one gives the temperature influence, introducing the constant D_5; Δ_ε is the strain modification for an element (when using finite element method).

The material is accepted to be intact (not broken, even locally) until the failure factor, D, calculated with relationship (3.2), is 1. At this time, the finite element cracks, debonding or detachment is started and an immediate post-failure answer is activated. This constitutive material model could only be used for solid, continuous bodies [71].

3.3. The Model for an Impact Projectile - Ballistic Stratified Panel

3.3.1. The Involved Bodies and the Model Conditions

The finite element model consists of two components, a bullet made of two solid bodies (jacket and core, each of different metallic alloy), a "perfectly bonded" connection between them and a panel with different numbers of layers (8, 10, 12, 16 or 24).

The panel has an area of 120 mm x 120 mm. The actual panel, fabricated and tested by the author, has dimensions of 300 mm x 300 mm and variable thickness, depending on the number of layers; this area of 0.09 m^2 allowed to have 3 hits, at an equal distance between hit locations of 120 mm, as peaks of an equilateral triangle. Due to hardware features (that imposes the time

necessary for running the simulation), the author selected a single hit (fire) on a smaller surface (120 mm x 120 mm) of the protective panel (the target), being sufficient to notice that the delamination does not reach the edges of the panel.

For reducing the time of running the simulation, the projectile, drawn after the reference [66], was brought very close to the panel front surface, the distance from the bullet tip to the panel surface is 0.258 mm.

The connection between each pairs of two panel layers is "bonded", the user may select the condition of debonding, namely "breakable", this nodes' detachment is initiated by reaching a value for tensile stress and shear stress. These characteristics are asked in the cohesive zone model with zero thickness (CZM) 70]. For these modelled panels, based on datasheet of the epoxy resin, the user selected the following values: 90 MPa for the tensile stress and 60 MPa for the shear stress.

For this finite element model, it was selected the breakable option, set with the "Stress Criteria". Then the connection may be broken during the analysis. The breaking criterion of two consecutive layers of the panel is defined as follows:

$$\left(\frac{\sigma_n}{\sigma_n^{limit}}\right)^n + \left(\frac{|\sigma_s|}{\sigma_s^{limit}}\right)^m \geq 1 \tag{3.4}$$

where $\boldsymbol{\sigma_n^{limit}}$ is the value for the limit at break for normal stress (in this model n is the value of the exponent in the relation (3.4), for the ratio of normal stresses n = 2), $\boldsymbol{\sigma_s^{limit}}$ is the value for the shear limit at break, m being the value of the exponent in relation (3.4), for the shear stress ratio, (m=2).

The interaction between solid bodies involved in this model is considered taking into account the friction. The friction coefficient is meant to be constant, COF = 0.1. The value of coefficient of friction in case of impact is heavy to be evaluated, the literature presenting only experimentally determined values for lower speeds than those characterizing the ballistic impact. Values of friction coefficient given in the literature are from 0.1 to 0.4 [33], [46]. In reality, in the impact process, the COF is not a constant value and it depends on friction couple of materials and the pressure in contact.

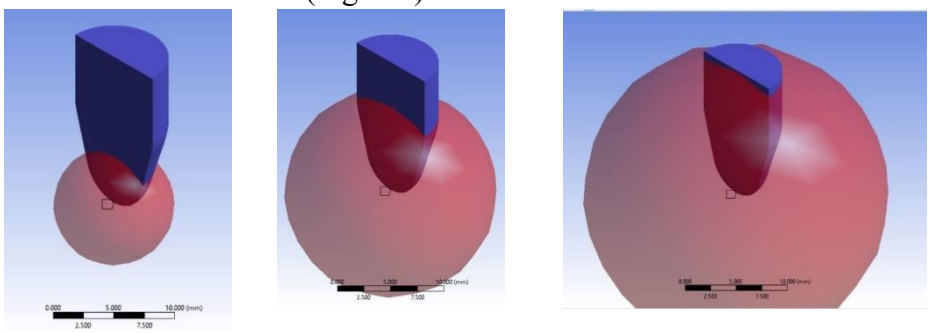
3.3.2. Mesh Network

The discretization network was done after a documentation on the subject, from which it resulted that the element size and the style of

discretization (including element type) is important, but these aspects have be adapted to the particular case [28].

For the projectile, the initial discretization network is built with at least two tetrahedral elements on the jacket thickness, over which finer discretizations are developed, with 3 influencing spheres, with radii of 5 mm, 10 mm and 15 mm, respectively, are overlapped in order to have a smaller increasing of discretization network elements. For the sphere of 5 mm radius, the size of the element is 0.35 mm, for the second sphere (of 10 mm radius), it is 0.45 mm and for the last sphere (of 15 mm radius), this parameter is 0.55 mm (Fig. 3.1).

Each layer of the protective panel has 0.8 mm in thickness (the same as the actual layer, with quadriaxial glass fibres, used to fabricate the composite in the laboratory). Each layer has only one element on thickness and the size of this element is 0.8 mm (Fig. 3.2).



a) Sphere with 5 mm radius

b) Sphere with 10 mm radius

c) Sphere with 15 mm radius

Fig. 3.1. The influence spheres for refining the mesh network for the bullet

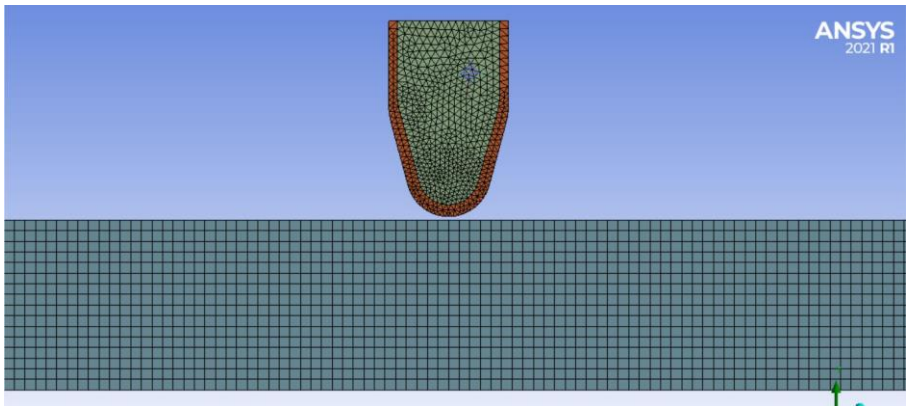


Fig. 3.2. Discretization network for the model run in this simulation of the impact bullet – stratified panel

The simulation includes an initial condition, for these cases, the user imposed the bullet velocity just before touching the panel (v_0 = 375 m/s), this velocity being the average measured value for the fires on the actual panels.

The model contains a plane of symmetry that passes the center of the square that defines the panel area and is parallel to panel side (and also contains the longitudinal section of the projectile axis).

The panel was fixed on the lateral surfaces of each layer.

3.3.3. Material Models of the Bodies Involved in the Model

In the simulations here-presented, the Johnson-Cook model was used for the projectile core material (a lead alloy) and its jacket material (a brass alloy), based on the experimental values reported by [13], [26], [55] (Table 3.1).

Table 3.1. Mechanical properties for materials the projectile jacket and core are made of

Property	Jacket (brass alloy)	Core (Lead alloy)
Density *[kg mm^-3]*	8.45e-006	1.135e-005
Specific heat at constant pressure *[mJ kg^-1 C^-1]*	380	1.288e+005
Young modulus *[MPa]*	90000	16000
Poisson coefficient	0.344	0.44
Temperature *[°C]*	22	22
Constants for Johnson-Cook constitutive model		
Initial yield limit *[MPa]*	90	1
Hardening constant *[MPa]*	628	55
Hardening exponent	0.72	9.8e-002
Constant of strain rate	0.266	0.231
Exponent for thermal softening	604	221
Melting temperature *[°C]*	927	327.5
Plastic strain rate (/sec)	1	1
Echivalent plastic strain at break (EPS)	0.4	0.4

The mechanical characteristics of each layer of the panel are given in Table 3.2.

Table 3.2. Mechanical characteristics of a layer

Property	Value
Density *[kg mm^-3]*	1.904e-006
Specific heat at constant pressure *[mJ kg^-1 C^-1]*	6e+005
Young modulus *[MPa]*	50000
Poisson coefficient	0.3065
Temperature *[°C]*	22
Isotrope bilinear hardening model	
Initial yield limit *[MPa]*	550
Tangent modulus *[MPa]*	10000
Temperature *[°C]*	22
Equivalent plastic strain at break	0.09

There are two reasons that recommend to use an isothermal model. Ansys Explicit Dynamics [71] does not use adiabatic models for dynamic processes and from literature, it could be accepted that, for the range of impact velocity 100-450 m/s, the thermal influence on mechanical behaviour of the model may be neglected in impact failure simulation.

Table 3.3. Characteristics for modeling interlaminar delamination

Temperature, °C	Maximum normal tensile stress, MPa	Normal displacement jump at completion of debonding, mm	Maximum tangential traction, MPa	Tangential displacement jump at completion of debonding, mm	Ratio
22	70	5	50	0.1	0.3

The CZM (cohesive model zone of zero thickness) was introduced between layers, in a way similar to reference [70], the name in Ansys Explicit Dynamics for modeling the CZM being "Bilinear for interface delamination" (Table 3.3) [71]; the failure criterion was set for “Fracture energies based debonding” (Table 3.4), for crack opening mode I.

Table 3.4. Values for energy at break in delamination

Temperature [°C]	Maximum normal contact stress [MPa]	Critical fracture energy for normal separation [J/m^2]	Artificial damping coefficient [s]
22	100	3000	0.1

3.4. Results of Simulation and Discussions

3.4.1. The Aim of Simulations

The model and simulations were performed to highlight the following aspects:

– the possibility of modeling the impact at macro level, with layers with isotropic characteristics, acceptable simplification because a layer has 4 oriented sublayers (0°/45°/90°/-45°), which gives some uniformity to the mechanical characteristics, at least in terms of fabrics, so that, on the basis of validation criteria, the model could be used to evaluate the ballistic resistance to a higher level than the one already tested,

– the validation criteria are: qualitative (penetration hole shape, delamination shape) and quantitative (number of broken layers on the impacted panel and maximum size of delamination, observable on the model back).

In this study, the influence of the number of layers and the influence of the impact velocity, for the same projectile, 9 mm FMJ, were discussed.

Runs were done for the following cases:

– number of layers: 8, 10, 12, 16 and 24; it should be noted that the actual tests were performed only on 8-, 16- and 24-layer panels, but the simulation would allow for assessing intermediate values of the number of layers, which would lead to a decrease in specific surface density, for a protection against the same threat,

– initial velocity was set for 375 m/s and 420 m/s; the higher velocity (for which there are no laboratory tests) would correspond to a higher level of protection (FB3) and the analysis of the simulations would allow an assessment on the basis of which a future test campaign for the higher level can be programmed.

The 10- and 12-layer panels did not be included in the actual test campaign, but the simulation can provide useful information on the impact resistance of the composite between tested values for the 8- and 16-layer panels, thus, an optimization of specific weight of the protection panel could be done in the virtual environment, following by testing only the panels, for which the thicknesses had been already considered effective in the simulation.

After the simulations, the failure processes in the virtual environment were compared to those obtained on the tested panels. The equivalent stress

distributions on each layer were analyzed using the "Path" function in Explicit Dynamics (exemples are given in Fig. 3.3) and compared for different panel thicknesses, obtaining the influence of the number of layers on the evolution of the equivalent stresses over time, on a layer of interest. Images (moments) belonging to the stages of the impact process can be extracted from the simulation.

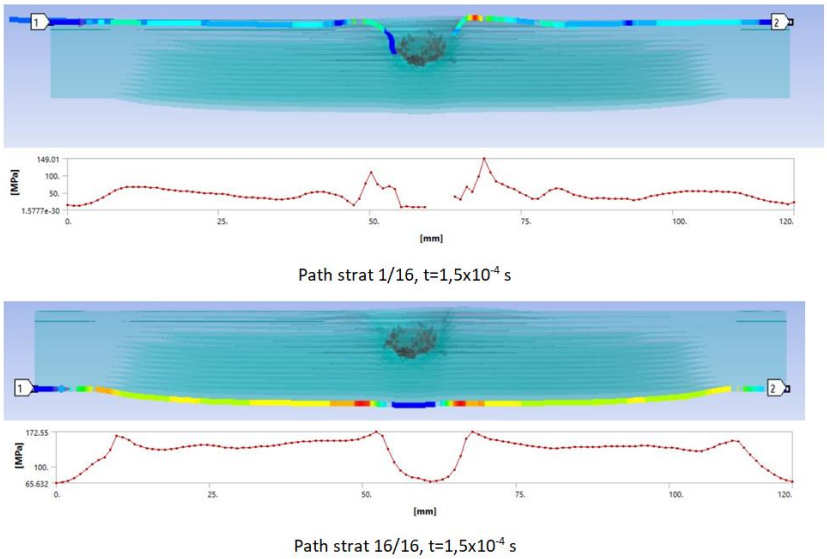


Fig. 3.3. Analysis of equivant stress on a single layer, at a certain time moment

For total penetration (8-layer panel) (Fig. 3.4), the stages observed in simulation are:

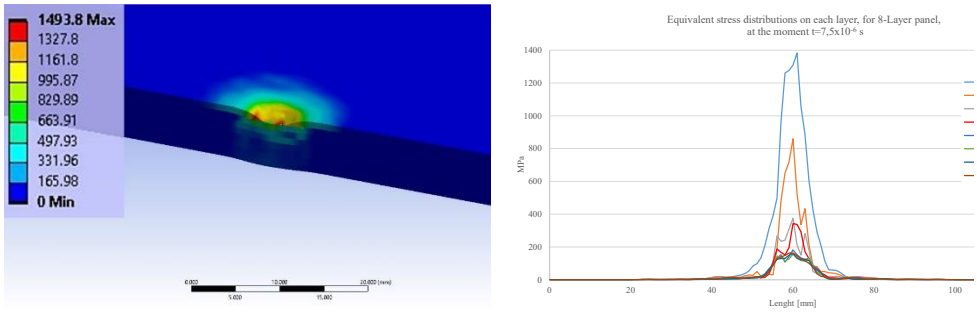
- the tensioning of the layers without breaking is a very short time stage, on this simulation only at the moment 7.5×10^{-6} s no broken layers are observed, but the values of the equivalent stresses reach high values, close to limit at break of the layer (1490 MPa in Fig. 4. a), and the first layer is strongly deformed by compression,

- from the moment t= 1.5×10^{-5} s, the break of layer 2 and 3 is initiated and the delamination between layers 1-2 and 2-3 could be noticed; there is also a beginning of delamination in the central area, where the deformation of the last layer is large,

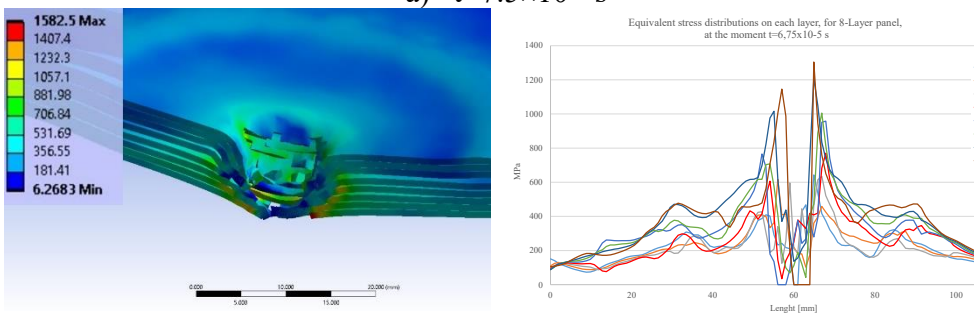
- a stage during which all layers are broken successively (here between 2.25×10^{-5} and 6.75×10^{-5} s),

- a stage in which the bullet continues to advance towards the panel, friction being generated between the bullet and the fragments of panel and bullet, even if it was damaged (deformed, scratched), it produces strong bendings of the edges of the penetration channel, already broken, resulting in small fragments.

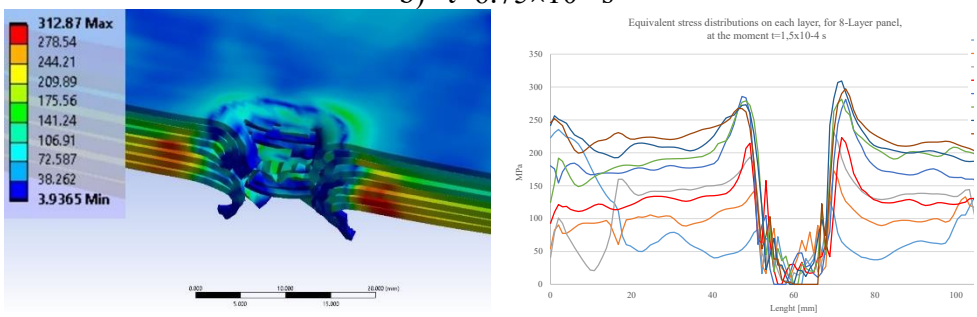
In graphs, the break of a layer is reflected by the equivalent stress decreasing to zero.



a) $t=7.5\times10^{-6}$ s



b) $t=6.75\times10^{-5}$ s



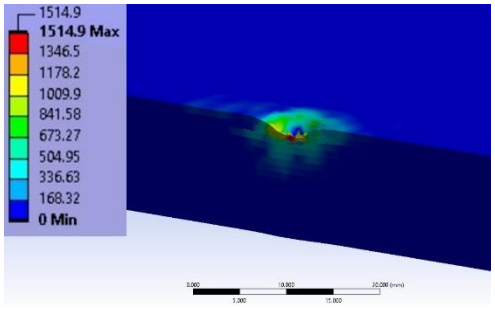
c) $t=1.5\times10^{-4}$ s

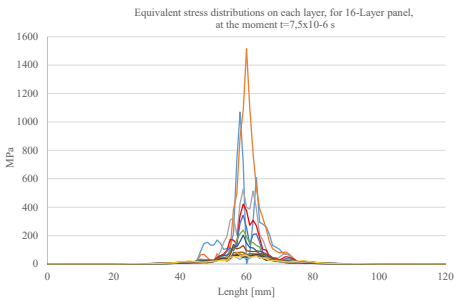
Fig. 3.4. Important moments during the impact process, for the 8-layer panel (that had a total penetration at the end of the simulation)

The graphs have no symmetry with respect to the axis of the projectile because the break of layers is not identical in section. This is explained by the local asymmetry of the initial discretization network and the contact conditions. In reality, there is no symmetry of the penetration orifice in an isotropic material due to various causes, including local differences in composition, structure, deformations etc.

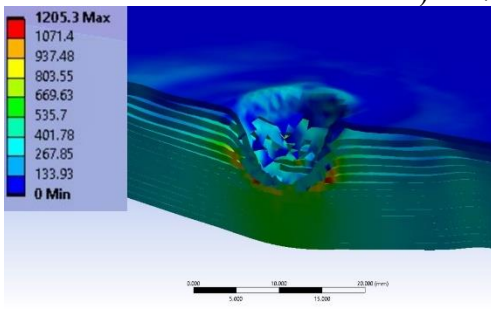
Towards the final moments of the impact, high stresses appear as stress concentrators on the edges of the fragments strongly bent due to the passage of the projectile; as the projectile advances and leaves layers, these ones have lower and lower stresses. See, for example, the equivalent stress distribution for layer 1, for t = 1.5×10^{-4} s in the graph in Fig. 3.4.

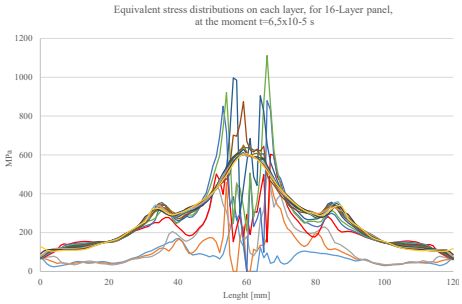
For partial penetration (16-layer panel) (Fig. 3.5), on this simulation, the tensioning of the layers without breaking is a very short stage, only at the moment 7.5×10^{-6} s no broken layers are observed, but the values of equivalent stresses reach high values, close to strength at break (1520 MPa for layer 2, in Fig. 3.5a). At the end of the simulation, the bullet is stopped between layers 4-5 and, for the other layers, the graph of equivalent stress is approximately similar.



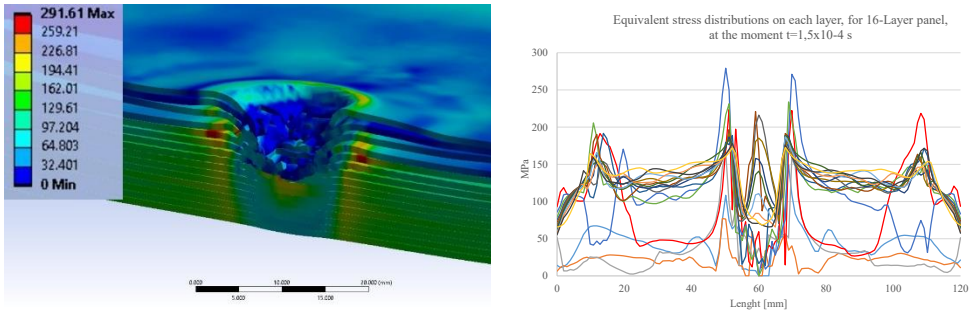


a) t=7.5×10^{-6} s





b) t=6.75×10^{-5} s

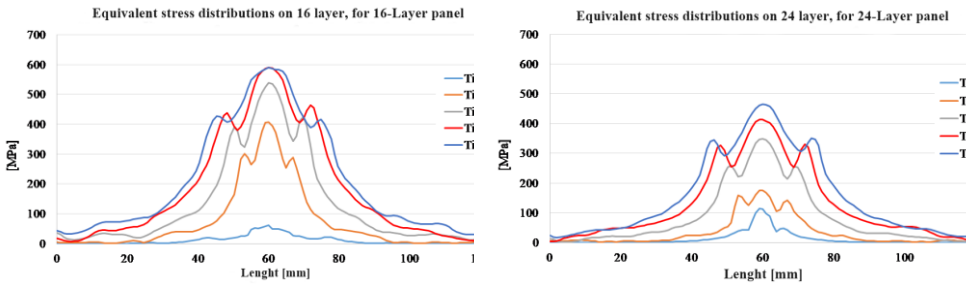


c) $t=1.5\times10^{-4}$ s

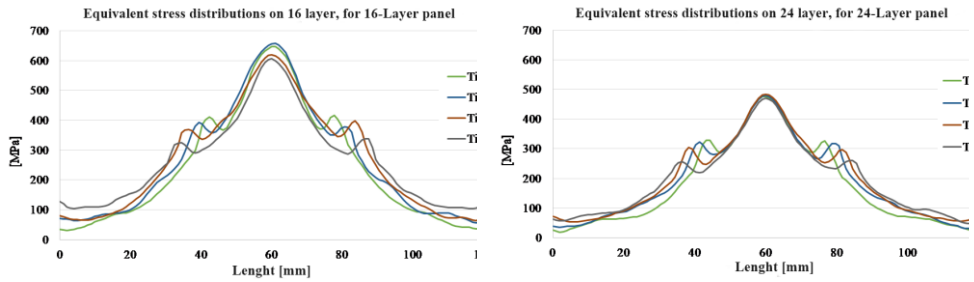
Fig. 3.5. Important moments during the impact process, for the 16-layer panel (with partial penetration)

Figure 3.6 shows the grouping of the equivalent stress graphs on the last layer, for the 16-layer panel and Figure 3.7 shows the same graphs for the 24-layer panel. There are similarities and differences between the two figures, although the qualitatively established stages are the same. The graphs marked with a) show that, at the first moment of the simulation (7.5×10^{-6} s), the maximum value for equivalent stress is obtained at 24 layers (110...115 MPa), higher than at the 16-layer panel (60...80 MPa), probably due to the elasticity of the thinner panel. For the last moment of this stage, higher values are found on the 16-layer panel (600 MPa) and 460 MPa on the 24-layer panel.

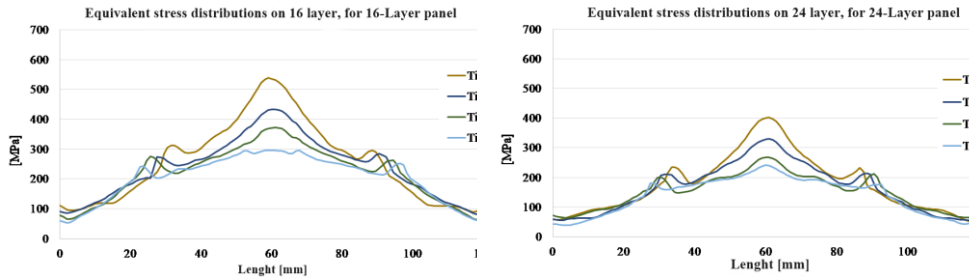
The graphs for the next two steps (b and c) are similar, and the same values are obtained on both analysed panels. Differences in shape appear only in the last stage, the thinner panel having a more tense area (see the equivalent stress distributions) under the projectile.



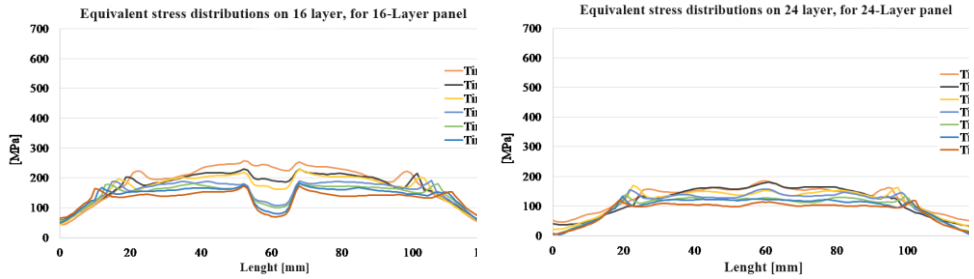
a)



b)



c)



d)

Fig. 3.6. Layer 16 from 16-layer panel

Fig. 3.7. Layer 24 for 24-layer panel

The time interval studied in the simulation (1.5×10^{-4} s) does not represent the whole impact process, i.e. the time interval at the end of which the involved materials are no longer tense or very slightly tense (with residual stresses) and the bodies are in rest.

3.4.2. The Influence of Impact Velocity on the Modeled Panel

The tests performed can be included in the FB2 level, but it was observed that for 16- and 24-layer panels, the number of broken layers is relatively small, 3...4 layers for the 16-layer panel (18.75%...25% of the number of layers) and also 3…4 layers for the 24-layer panel (which represents 12.5%...16.6% of the number of layers for this panel).

These small values suggest that these panels could be tested at a higher level to see if they resist. The simulation for the average velocity at FB3 level, 420 m/s, could be useful in the sense that the results would be a starting point in determining whether or not it is worth doing tests at this higher level.

The following figures (Fig. 3.8 to Fig. 3.10) show a comparison between the equivalent stress distributions for the 8-, 16- and 24-layer panels, at impact velocity v_0 = 375 m/s and v_0 = 420 m/s. The aim of this comparison is to evaluate, on the run simulations, whether the analyzed panels could be subjected to tests at a higher level (FB3). From the experimental data (see Chapter 5), there was noticed that, for 16-layer and 24-layer panels, the "reserve" of layers, the non-perforated layers, is relatively high and would suggest a ballistic resistance to more dangerous threats.

Figure 3.8 gives the equivalent stress distributions at the first moment of the simulation (t = 7.5×10^{-6} s). The increase in velocity has led to substantial changes in stress distribution, when using the same projectile.

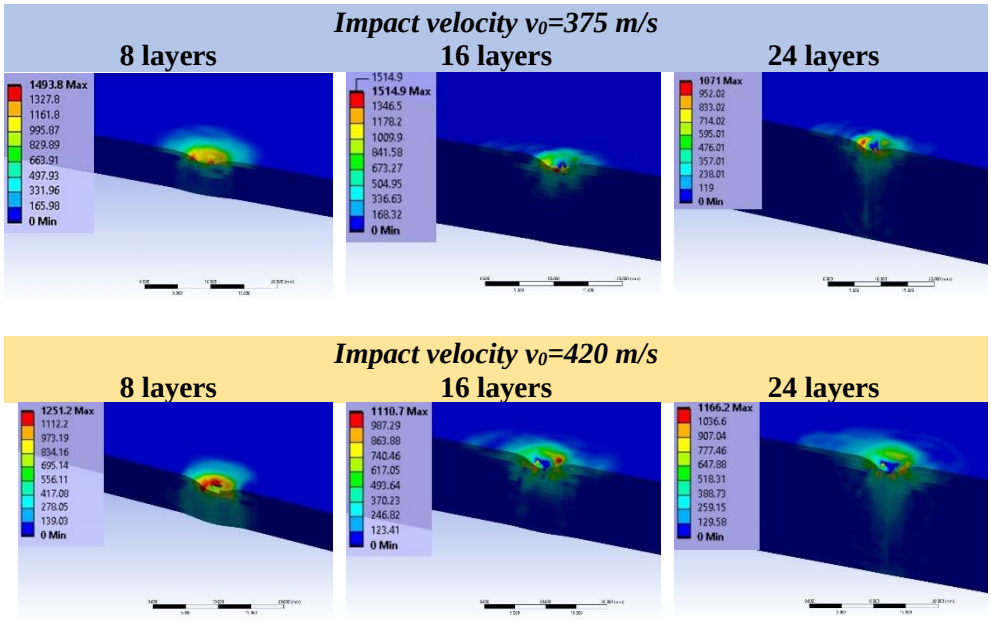


Fig. 3.8. Distributions of equivalent stress, at time moment t=7.5×10^{-6} s, for panels of different number of layers

For panel with 8 layers, the higher impact velocity has already induced the break of the first layer and the initiation of small delamination, as size, between layers 1-2 and 2-3. At the lower velocity, the last 4 layers are not stressed yet, while at v_0 = 420 m/s, a cylindrical equivalent stress distribution

of the order of 100-200 MPa is observed until the last layer. This increase in the most loaded areas is also observed on 16-layer and 24-layer panels. Delamination is more pronounced at higher velocity and it occurs between several pair of layers (1-2, 2-3).

For thicker panels, there is a tendency for the bullet to break fewer layers as compared to those in the 8-layer panel. The difference is that, at lower velocity, the number of broken layers is smaller. Delamination is no longer visible on the lower layers, but the separation between the layers is higher at higher velocity.

For thicker panels, the difference is in the development of delamination, in the cross section of the panel, and the projectile destroyed 1-2 extra layers for higher velocity.

For t = 7.5×10^{-5} s (Fig. 3.9), the 8-layer panel is already completely perforated, but at higher velocity, the damage is more aggressive and the hole is larger. Also, at this velocity, there are larger bendings of the last back layers. For the 16-layer panel, the lower velocity destroyed 6 layers, and for the velocity of 420 m/s, there were destroyed 8 layers.

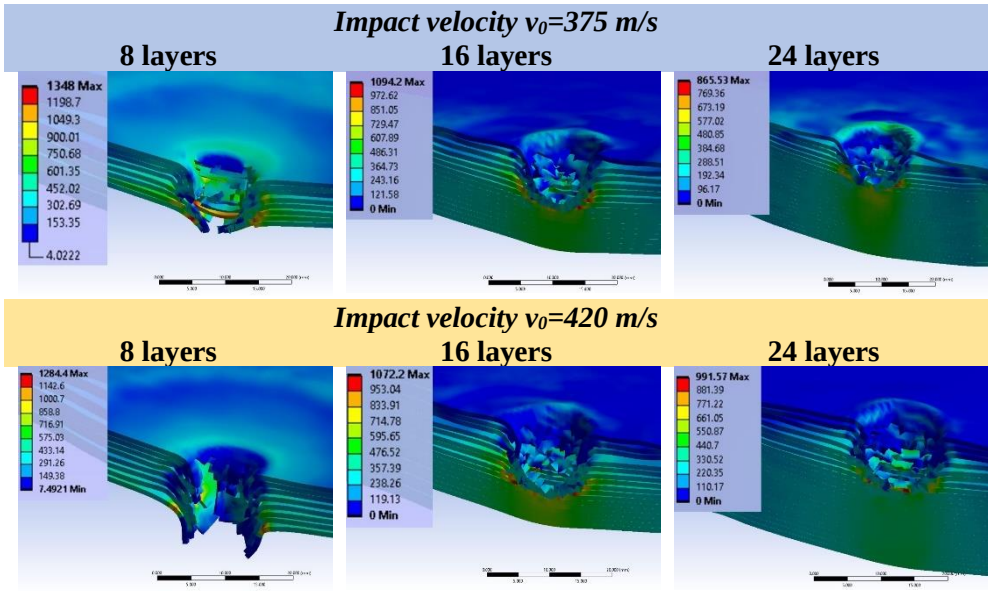


Fig 3.9. Equivalent stress distributions, at time moment t=7.5×10^{-5} s, for panels of different number of layers (color scale is given for each image)

The same trend is maintained for the 24-layer panel (4 layers broken at v_0 = 375 m/s and at v_0 = 420 m/s, 6 layers are broken).

For the 8-layer panel, at low speed, the bullet still rubs against the last layers, while at higher velocity, it has already left the contact area with the panel.

The analysis of the last moment in simulation (Fig. 3.10) shows stresses below the yield limit, for both velocities and all panels, but the moment captures the fragmentation of the last layers for higher velocity, for the 8-layer panel. For partially penetrated panels, differences in appearance are very important.

At impact velocity of 375 m/s, the 16-layer panel has 5 layers destroyed, which represents 31.2% of its thickness. At impact velocity of 420 m/s, the same panel had 12 layers destroyed, which represents 75% of its thickness. In some references [18], a panel is considered advisable if its "reserve" (the material that remains intact) is around 30% of its thickness. It turns out that this 16-layer panel would not be advisable, or more tests would have to be done to confirm or disprove the simulation. Taking into account the same criteria, the 24-layer panel would cope with the projectile at higher velocity (420 m/s), because the broken layers represent only 25% of the panel thickness.

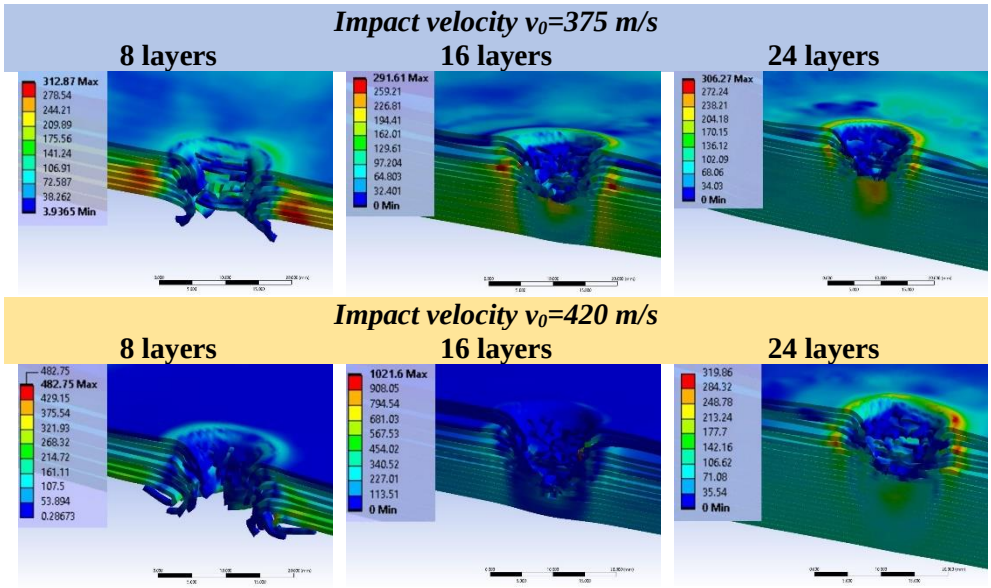


Fig. 3.10. Equivalent stress distributions at time moment $t=1.5\times10^{-4}$ s, for panels of different number of layers (color scale is given for each image)

According to the simulation results, it is likely that a panel with a smaller number of layers (20-22 layers) will also meet the protection requirements, at an impact velocity of v_0 = 420 m/s, but it will have a lower

surface density. It should be emphasized that these modeling results can only be put into practice after laboratory tests, according to the standards in force; extrapolating the results from modeling directly to the product is not accepted in this high risk domain.

3.4.3. Simulation of a Panel Thickness Range, for v_0 = 375 m/s

This analysis was done in order to argue for an intermediate design solution (as concerning the number of layers) between two other solutions already modeled and confirmed by laboratory tests. The idea is that a surface density as low as possible would be more effective in terms of weight, price and manoeuvrability, without affecting the level of the panel's protection for the same threat.

Experimentally and numerically, there are two variants of this protective panel, with extreme behaviours:

- the panel of 8 layers, with complete penetration (which is not accepted in ballistic protection),

- panel with 16 layers that has withstood laboratory tests well and whose failure is simulated with a high degree of likelihood.

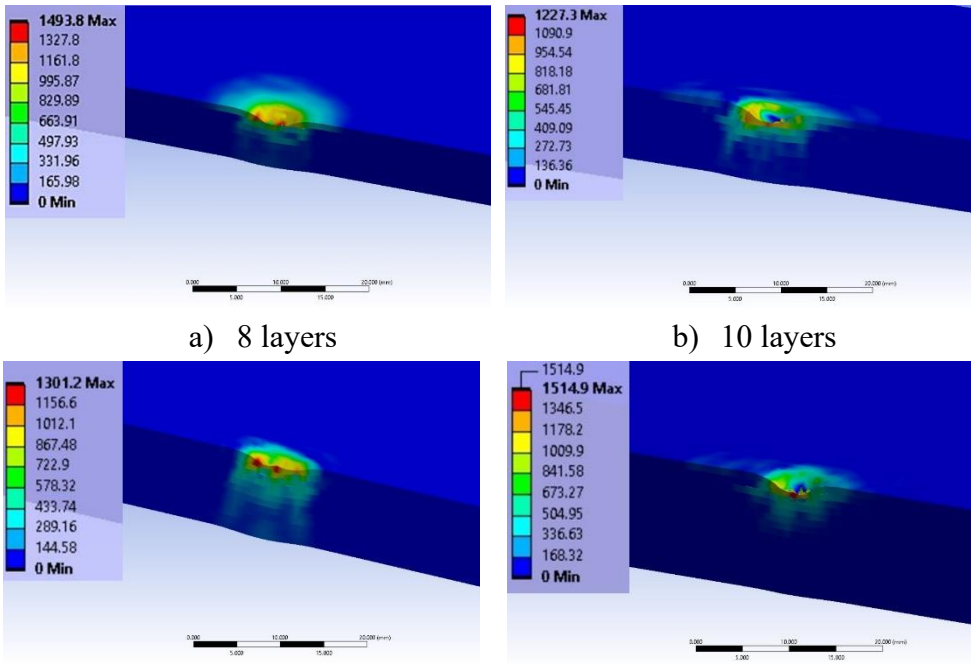
The question that this analysis would answer is: in the interval of 8-16 layers, is a panel with the layers' number less than 16, but could have the performance that deserves to be tested and, then, proposed as a prototype? It was also run two more cases involving the same bullet on panels with 10 layers and 12 layers, respectively, in order to see if one of these two case, or both, could be candidate for being tested in laboratory.

The next figures show the panel, at the same moment of the projectile impact simulation. The projectile is visually hided (transparent) in order to point out the failure processes of panels.

At the initial time moment of the simulation ($t = 7.5\times10^{-6}$ s), the equivalent stress distribution is samblable, the bullet impact generating local areas with high stress values (Fig. 3.11).

The equivalent stress values are better noticed in the graphs for layer 1, on each analyzed panel, given in Fig. 3.12. The side length of each modelled layer is 120 mm, the middle value of 60 mm being positioned at the bullet axis and having the impact direction (this direction is also perpendicular to the protective panel surface). The panels characterized by a greater thickness (12-layer panel and 16-layer panel) show minimum values of von Mises stress in the contacted area under impact. The value of zero is considered for (for instance, for the panel with 16 layers) the local break of the layer. Values slightly above zero (for instance, 60…70 MPa for the panel of 10 layers)

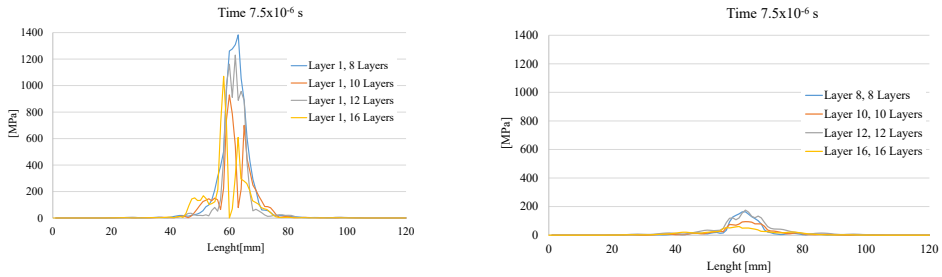
suggest that the time of local break is around the moment under consideration. For these minimum values, the rupture is possibly not located in this analyzed symmetry plane, but somewhere in front or in the back of the symmetry plan of the analysis. The panels of 8 layers and 12 layers have the values of von Mises stress high. This implies that the local break of the layer has not yet initiated in the analyzed cross section of the model, at that moment.



a) 8 layers b) 10 layers

c) 12 layers d) 16 layers

Fig. 3.11. Equivalent stress distributions (in MPa), at moment t=7.5×10^{-6} s

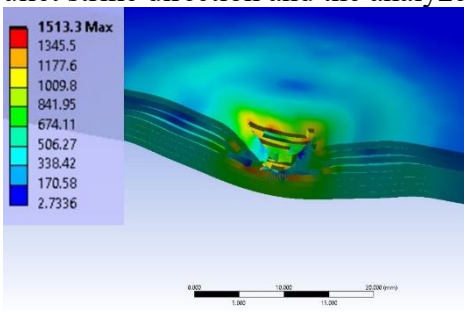


a) Layer 1 b) Last layer

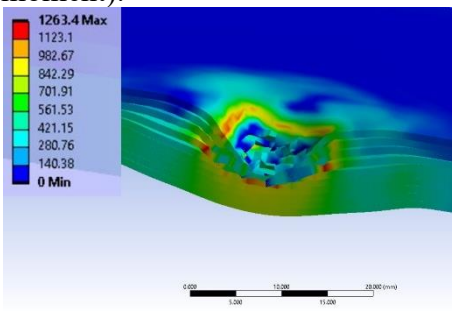
Fig. 3.12. Graphs of equivalent stress on layer 1 (a) and on the last layer (b), for different panels (t=7.5×10^{-6} s)

At moment t=3.75×10^{-5} s (see Fig. 3.13 and Fig. 3.14), maximum values for equivalent stress are at the contact edge between the bullet and the panel,

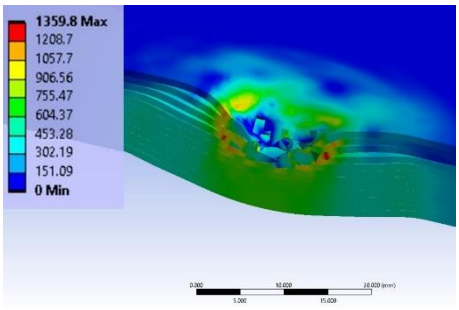
except for the panel of 16 layers. The higest values of the equivalent stress passed the yield limit characterizing the layer material (550 MPa). The red micro zones (meaning maximum values in each image of the simulation) are located either below the bullet or laterally because it laterally presses and pushes the layers. On the other panels there were generated maximums values of 700-800 MPa, except for the panel of 16 layers. Delamination is visible on all panels, more pronounced between first layers (taking into account the bullet strike direction and the analyzed moment).



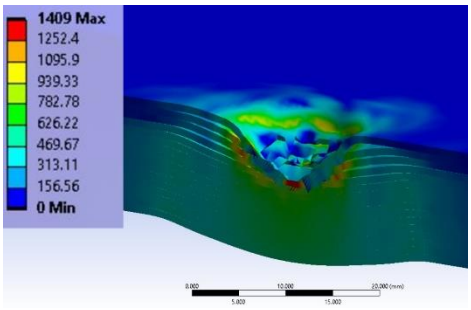
a) 8 layers



b) 10 layers

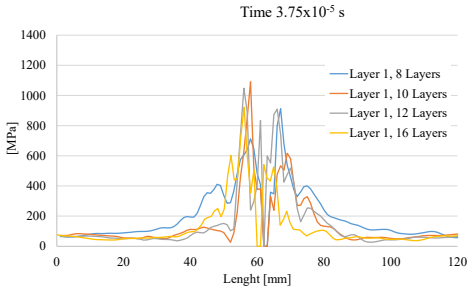


c) 12 layers

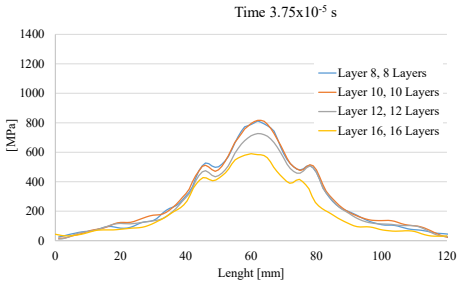


d) 16 layers

Fig. 3.13. Equivalent stress distributions (in MPa), at moment t=3.75×10^{-5} s



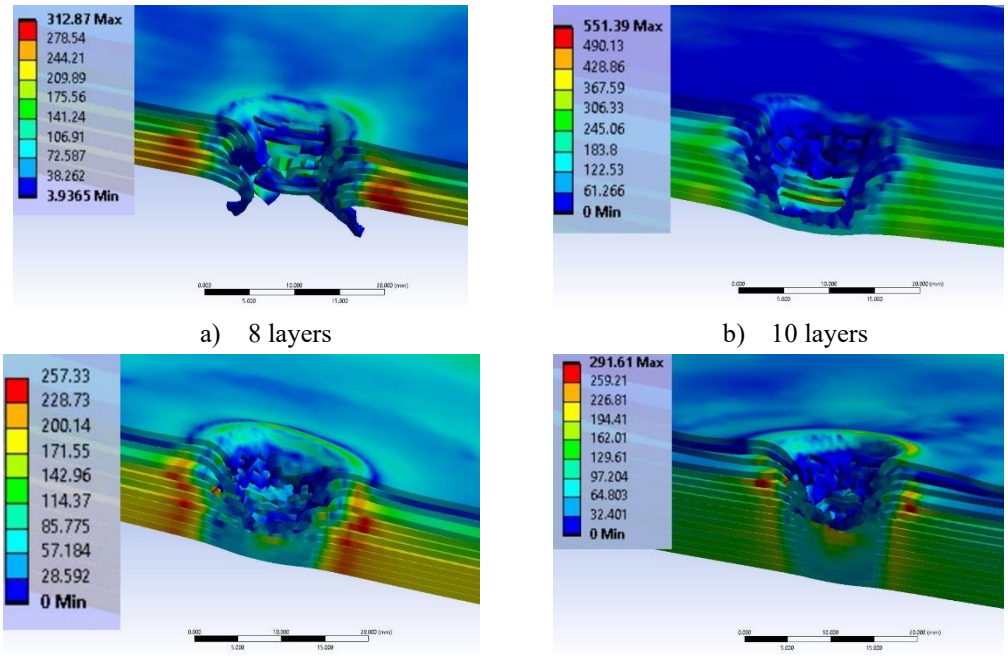
a) Layer 1



b) Last layer

Fig. 3.14. Graphs of equivalent stress on the central cross section, on layer 1 (a) and on the last layer (b), for different panels (t=3.75×10^{-5} s)

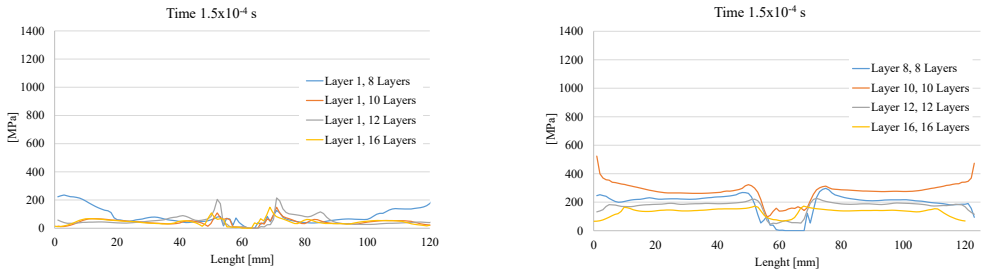
Both for layer 1 and the last layer, on each modelled panel, the values for the equivalent stress decreased to the simulation end. This observation is visible in Figures 3.15 and 3.16.



a) 8 layers b) 10 layers

c) 12 layers d) 16 layers

Fig. 3.15. Equivalent stress distributions (in MPa), at time moment $t=1.5\times10^{-5}$ s



e) b)

Fig. 3.16. Equivalent stress distributions (in MPa), for layer 1 (a) and the last layer (b), at the moment $t=1.5\times10^{-4}$ s

3.5. Conclusions

This section presents a finite element model for the impact bullet – stratified panel, at macro level (each layer of a panel is considered made of a homogenous and isotropic material), with the following aspects:

- the solid bodies and the materials they are made of behave in the elasto-plastic domain, with EPS (equivalent plastic strain at break) failure criterion [19], [41]; even if they are time consuming, the simulations accepting all bodies being deformable, these analyses are more realistic,

- the modeling of the delamination process by introducing the cohesive zone model with zero thickness,

- identification of the stages of the impact process, for complete and partial penetrations,

- simulations for the impact bullet - protective panels were validated based on realistic criteria: the number of broken layers, with an accuracy of ± 1 layer, and the size of delamination on the panel back (there were measured the circle diameters visible on the back of the actually tested panels and those visible on the back of the modelled panels),

- for intermediate thicknesses (panel with 8 layers and 16 layers), from laboratory test results, there was noticed a "reserve" of impact resistance, thus, the simulations could establish intermediate effective panel thicknesses, but smaller, for the same threat,

- running 5 cases at impact velocity 375 m/s (average value of the tests performed in the laboratory) and 3 cases at an impact velocity of 420 m/s, characteristic for FB3 level, with the same ammunition.

From the results obtained for these runs, the following conclusions could be drawn:

- although the layer constitutive material model was simplified to a isotropic hardening bilinear model, with values from the open-source literature, the results were validated by the number of layers broken for the partially penetrating plates and by the delamination size on the back of the last layer, for both cases of total and partial penetrations,

- based on the results for panels modeled and actually tested, cases with intermediate thicknesses were run; for panels with 10 layers and 12 layers, the numerical solution still offers a ballistic protection for this particular threat (9 mm FMJ with v_0=375 m/s); but this design and virtual solution should be validated by testing in the laboratory; if they provide good ballistic protection, they will have a lower surface density (implicitly, panel thickness), a better characteristic as compared to thicker panels.

Table 3.5 shows values of delamination size, on actually tested panels and on simulations. The largest difference in delamination diameters, of 29.4% as compared to value measured on panels tested in ballistic laboratory, was obtained for the panel of 8 layers, with complete penetration. This difference could have been caused to the higher elasticity of the actual panel and the fact that, when the bullet passed through the last layers, the separation between them was more severe. For the panel of 16 layers, a smaller difference of 10.1% was noticed between the actual protective panel and the simulated one, acceptable for these macro simulation conditions. For the thicker ballistic panel with 24 layers, the difference between diameters of delamination circles for the tested panel and the impact-simulated panel was 14.4%, the results being reasonably close to use the material model in other simulations, in not very large parameter ranges (for the impact velocity and the number of layers). Of course, these results could be taken into account only for one threat, represented by the bullet of 9 mm FMJ (full metal jacket)

Table 3.5. Diameters of the delamination circles on the tested panels (on their back faces) and on the models with the same number of layers

Panel	**Panel thickness (medie)**	**Actual panel**				**Diameter from the model**
		Diameter 1 fire 1	**Diameter 2 fire 2**	**Diameter 3 fire 3**	**Average diameter**	
	[mm]					
8 layers	6.37	165	165.9	158.09	**162.99**	**117.04**
16 layers	12.49	105.86	111.5	108.62	**108.66**	**100.19**
24 layers	18.26	102.17	100.6	98.14	**100.3**	**86.1**

Chapter 4. Laboratory-Scale Technology of Ballistic Protection Panels

4.1. The Involved Materials

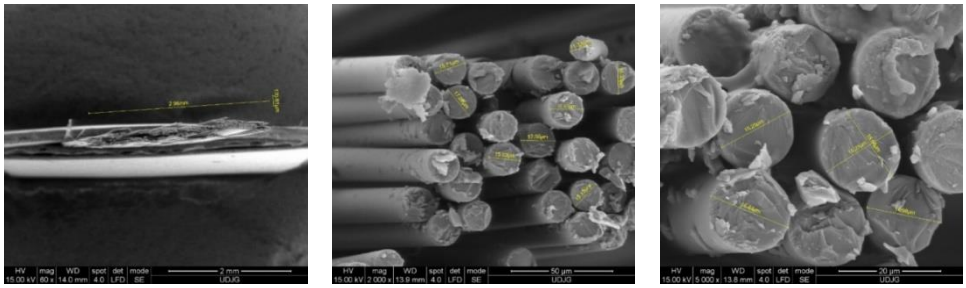
4.1.1. Glass Fibers and Glass Fiber Fabrics

The fabric used in this study is layered into four oriented substrates (0°/+45°/90°/-45°), which assumes from the start, that the fabric will have a quasi-isotropic behavior (Fig. 4.1). Trade name is 1200 g/m^2 Quatriaxial Glass Cloth (0°/+45°/90°/-45°), with the code WTVQX1200-1 E-glass, Q1200E10Q [80]. Table 4.1 details the architecture of the fabric reinforcement. Figure 4.1 shows the size of the glass fiber yarns, measured under a scanning electron microscope. The rolls of glass fiber fabric were kept in the laboratory at a relative humidity of 40-70% and a temperature of 18-30 °C, as recommended by the manufacturer. Polyester, vinyl ester and epoxy resins are compatible with this fabric. The water content is at maximum 0.2% by mass (according to ISO 3344).

Table 4.1. Architecture of the fabrics

The fabric architecture			
Layer	Yarn orientation	Fiber type	Area Weight
1.	0 °	600 Tex	283 g/m^2
2.	45 °	300+600 Tex	300 g/m^2
3.	90 °	600 Tex	307 g/m^2
4.	-45 °	300+600 Tex	300 g/m^2
5.	Stitch	76 DTex	10 g/m^2

Total: 1200 g/m^2 (±%3)



a) yarn dimensions b) measurement of the glass fiber diameter

Fig. 4.1. Dimensions of the yarn (a) and of glass fibers (b), measured using a scanning electron microscope

Figures 4.2-4.3 show basic EDX analyzes for the fabric used in this paper. Both cross-sections through the fiber and the fiber jacket were analyzed, punctually or in small rectangular areas (with a side of 2… 5 μm).

From Fig. 4.4, it is observed that boron, carbon, aluminum, silicon and calcium predominate, with traces of Fe, Zn and Ti, a composition that could be positioned between glass E and glass S, the particularity of the composition being assigned to the raw material extraction area.

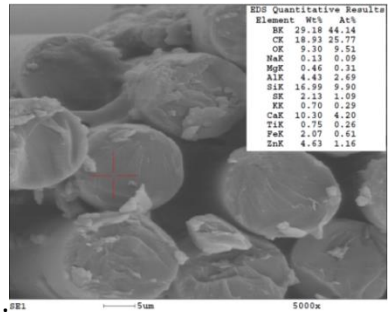


Fig. 4.2. EDX elemental analysis EDX of fibers (core)

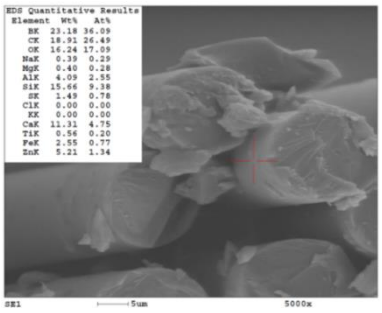


Fig. 4.3. EDX elemental analysis EDX of fibers (jacket)

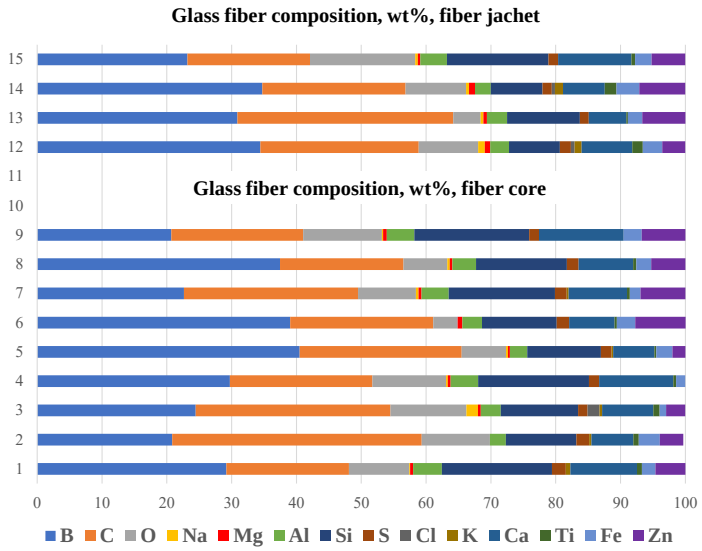


Fig. 4.4. Glass fiber composition, from EDX analysis

4.1.2. Epoxy Resin Matrix

After a documentation in the field of resins for fiberglass composites, from the experience of the contract team 725/2017 [22], I selected the two-

component resin Biresin® CR82 with hardener CH80-2, from the products offered by the manufacturer Sika Group [82].

The mixing ratio must be followed accurately, as given in the resin data sheet, for optimal results. Deviation from these reports will reduce performance. The final values for thermal and mechanical properties depend on the treatment cycles after aging.

Biresin® CR82 is an epoxy resin for individual, manual lay-up, layer forming, vacuum forming and winding, especially for applications where heat treatment temperature ≥ 75 °C cannot be applied. It can be used in marine and general composites for industry. The material and processing are recommended to be from 18 °C to 35 °C [74].

Table 4.2 shows the family of suitable hardeners for Biresin® CR82 resin. The Sika Company (through PolyChem Bucharest) offers 4 hardeners (B) with a single mass mixing ratio for each. Biresin® CH80-1 and CH80-2 hardeners can be removed from the mold at room temperature. Table 4.3 shows mechanical and thermal properties of the already formed and heat-treated resin and it is observed that using the hardener CH80-2, a fairly high tensile limit is obtained. I did not choose the CH80-1 hardener, which has a strength limit only 5% higher than the resin obtained with the CH80-2 hardener.

Table 4.2. Characteristics of resin Biresin® CR82 and hardeners

Characteristics		Resin (A)	Hardener (B)			
Individual Components		Biresin® CR82	Biresin® CH80-1	Biresin® CH80-2*	Biresin® CH80-6	Biresin® CH80-10
Mixing ratio	Weight	100	27			
	Volume		32	31	32	32
Viscozity, 25°C	mPa.s	~1.600				
Density, 25°C	g/ml	1.11	0.95	0.99	0.95	0.95
			Mixture			
Potlife, 100g/RT, (approx.)		min	80	80	220	330
Mix viscosity, 25°C (approx.)		mPa.s	850	600	400	390

* The hardener used for the panel fabrication

Table 4.3. Mechanical and thermal properties of the resin

Typical mechanical properties of fully cured neat resin						
Resin **Biresin® CR82** (A)	With hardener **Biresin®** (B)		**CH80-1**	**CH80-2**	**CH80-6**	**CH80-10**
Tensile strength	ISO 527	MPa	94	90	84	82
Tensile elasticity modulus	ISO 527	MPa	3000	3000	2900	2900
Elongation at break	ISO 527	%	4.9	5.6	6.4	6.2
Flexural strength	ISO 178	MPa	140	130	127	118
Flexural modulus	ISO 178	MPa	3300	3200	2900	2800
Compressive strength	ISO 604	MPa	120	105	110	110
Density	ISO 1183	g/cm^3	1.14	1.14	1.14	1.14
Shore hardness	ISO 868	-	D 85	D 85	D 85	D 85
Impact resistance	ISO 179	kJ/m^2	38	66	55	56
Typical thermal properties of fully cured neat resin						
Resin **Biresin® CR82** (A)	With hardener **Biresin®** (B)		**CH80-1**	**CH80-2**	**CH80-6**	**CH80-10**
Heat distortion temperature	ISO 75A	°C	93	83	71	71
Glass transition temperature	ISO 11357	°C	97	90	83	85

An adequate heat-treatment cycle could be as following:

- heating rate of approx. 0.2°C/min till approx. 10°C bellow the glass transition temperature, Tg,
- maintaining in mold at this temperature for 2 hours to 12 hours,
- the resulted composite will be cooled with ~0.5°C/min.

The cooling stage will be adapted to manufacturing and financial resources. Using the hardeners (B) Biresin® CH80-1 and CH80-2, the composite could be extracted at room temperature from the mold.

4.2. Laboratory-Scale Technology for Obtaining the Designed Panels

The purpose of the technology is the laboratory-scale production of ballistic protection panels coded (OGe) (Fig. 4.6), intended for light armor for vehicles and protected enclosures. The panel can be integrated into protection systems. The advantage of the proposed technology is that panels of different

thicknesses can be made with the same steps and with characteristics in a narrow range (for example, the fibers mass concentration, allowances of thicknesses, etc.).

The cutting process was carried out with the help of an electric scissors, brand Vibromat S-54 , with a cutting diameter of the disk having 50 mm, the weight being 700 g, the output power 80 W and the maximum cutting height of the layers being 12 mm. Only one layer each was cut.

The work laboratory was organized as follows: a work stand for cutting fiberglass fabrics and another stand (including the press and the hydraulic winch and the brushing place) for the manufacture of OGe panels (Fig. 4.7).

Mixing the resin components. Because of the particular laboratory work, a mixture of 800 g of CR82 resin and 200 g of CH80-2 hardener was mixed for panels with more than 16 layers and mixtures of 400 g of CR82 resin and 100 g of CH80-hardener each, for panels with less than 16 layers. Weighing the resin components and panels was done with a precision electronic scale.

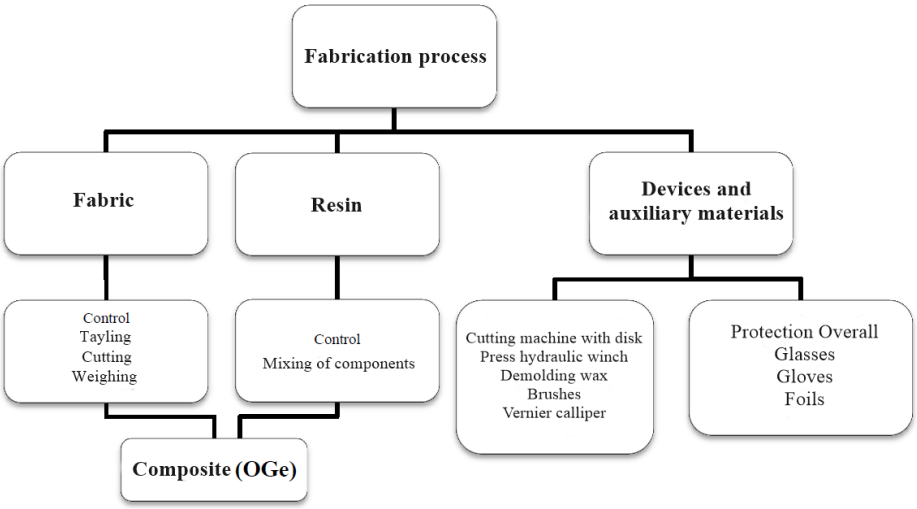


Fig. 4.6. Diagram of the laboratory scale technology for producing the composites



Fig. 4.7. Organization of the laboratory for manufacturing the panels

A layer of extraction wax is applied to the surface of the mold and the plywood sheets to ensure that the composite comes off the mold more easily. A thin layer of wax is also applied to these sheets. CIREX CP 10 is an extraction wax (Airétec supplier, RomPolimer Composites distributor), used for polyester resins and epoxy resins.

The laying-up process consists in spreading the resin, on each layer, with the help of a brush (Fig. 4.8).

The ballistic protective panels were kept in the press under load, for at least 8 hours (Fig. 4.9).

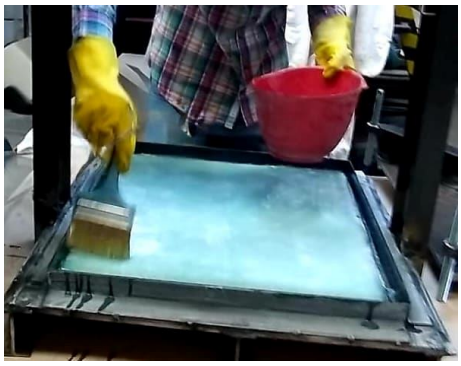


Fig. 4.8. Laying-up process of layers with the mixture resin+hardener



Fig. 4.9. The press for fabricating the panels coded OGe

Once the hardening process is complete, the panels are removed from the press and after that edge finishing operations are required, without affecting the reinforcing area. After finishing the panel edges, the composite was checked for integrity, weighed and coded (Fig. 4.10).

Aging consists of maintaining the panels at the room temperature, for 7 days.

The heat treatment was carried out after the natural aging, in two stages, taking into account the software of the used oven, of 3 hours each, at 60 °C, in the oven at Dunărea de Jos University of Galați, Faculty of Sciences and Environment, Department of Chemistry, Physics and Environment (Fig. 4.11).

Figure 4.12 shows the Gantt chart for scheduling the production of a set of 5 panels.

In laboratory-scale manufacturing, for a set of 5 plates, the time required to produce them is 12…13 days.

Conclusion. The processing time depends to a very small extent on the number of layers (laying-up and cutting operations depending on the number of operators responsible for this operation).

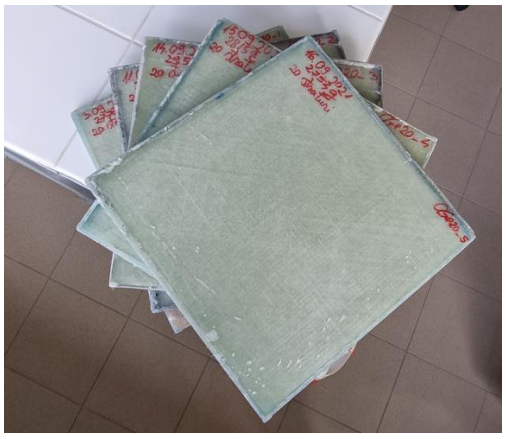


Fig. 4.10. A set of 5 panels, each one made of 20 layers



Fig. 4.11. Arrangement of the panels in the oven, with spacers made of wood, for the set of panels with 20 layers

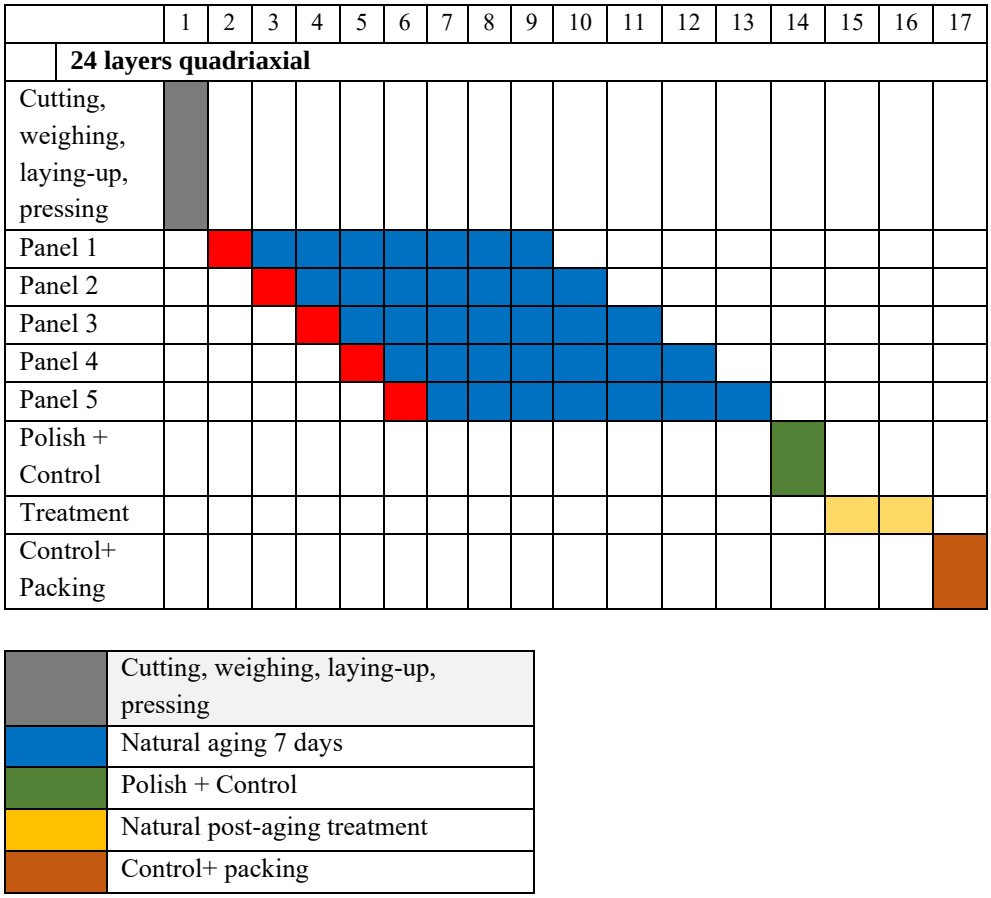


Fig. 4.12. Gantt Diagram for programming the manufacturing of a set of 5 panels, made of 24 layers

4.3. Characterization of Elaborated Panels

Based on the observations from the documentation and from some preliminary tests on 24-layer and 16-layer panels, the following sets of panels were produced: 3 panels made of 8 layers, 5 panels with 16-layer plates, 5 panels with 20-layer plates, 5 plates 22 layers, 5 panels with 24-layer boards and 3 panels with 32-layer boards.

For each set, the parameters in Tables 4.4...4.5 were calculated. Here, are presented here only data for 8- and 16-layer panels.

Table 4.4. Characteristics of the 8-layer panels

No.	Fabric mass	Panel mass	Resin mass*	Fabric/panel mass ratio**	Surface density***	Thickness in 4 points				
						1	2	3	4	Average
	[g]	[g]	[g]		[kg/ m^2]	[mm]				
0	1	2	3	4	5	6	7	8	9	10
Panel 1	840	1130	290	0.743	12.55	6.41	6.21	6.27	6.70	6.40
Panel 2	827	1112	285	0.743	12.35	6.23	6.46	6.20	6.62	6.38
Panel 3	837	1106	269	0.756	12.28	6.32	6.25	6.64	6.12	6.33
Average	**835**	**1116**	**281**	**0.747**	**12.39**					**6.37**
Max	840	1130	290	0.756	12.55					
Min	827	1106	269	0.743	12.28					
Standard deviation	**5.56**	**10.19**	**8.96**	**0.006**	**0.11**					**0.029**

* The resin mass = panel mass – frics mass, meaning (column 2 - column 1)

** Fabric/panel mass ratio = Fabric mass / Panel mass, meaning (column 1/ column 2)

*** Surface density = Panel mass /Panel surface (0.09 m^2)

Table 4.5. Characteristics of the 16-layer panels

No.	Fabric mass	Panel mass	Resin mass*	Fabric/panel mass ratio**	Surface density***	Thickness in 4 points				
						1	2	3	4	Average
	[g]	[g]	[g]		[kg/m^2]	[mm]				
0	1	2	3	4	5	6	7	8	9	10
Panel 1	1675	2145	470	0.780	18.61	11.71	11.84	11.37	11.93	11.71
Panel 2	1620	2230	610	0.726	18	13.22	12.78	13.51	11.95	12.86
Panel 3	1702	2315	603	0.735	18.91	12.31	12.94	12.84	13.52	12.90
Panel 4	1675	2220	545	0.754	18.61	12.47	12.43	12.51	12.56	12.48
Panel 5	1680	2195	515	0.765	18.66	11.84	13.45	12.05	12.62	12.49
Average	**1670**	**2221**	**549**	**0.752**	**18.59**					**12.49**
Max	1702	2315	610	0.780	18.91					
Min	1620	2145	470	0.726	18					
Standard deviation	**27.11**	**55.44**	**53.01**	**0.019**	**0.302**					**0.427**

* The resin mass = panel mass – frics mass, meaning (column 2 - column 1)

** Fabric/panel mass ratio = Fabric mass / Panel mass, meaning (column 1/ column 2)

*** Surface density = Panel mass /Panel surface (0.09 m^2)

4.4. Conclusions Concerning the Fabrication of the Panels

This chapter introduced an original laboratory-scale technology for obtaining ballistic protection panels.

The process has repeatability, precision and robustness. OGe panels have the dimensions 300 mm x 300 mm.

The recipe for making panels and laboratory technology is original.

The fabrication was done in compliance with the norms of safety and health at work, with adequate protective equipment.

The technological process of fabricating the OGe panel, of various thicknesses, includes the following phases,

- cutting the fabric layers (and weighing the cut layers that will be included in each panel),
- making the resin + hardener mixture,
- laying up the liquid matrix and overlapping the layers of fabric,
- pressing and controlling the thickness of the panel in press,
- heat treatment, maintenance at 60 °C, for 6 h (2 treatments of 3 h each),
- quality control (weighing, thickness measurement).

The characteristics of the elaborated panels are given in Table 4.6. Analyzing the values, small standard deviations and an almost constant fiber/panel mass ratio are noticed, regardless of the thickness of the plates. (average values are for 5 panels, except for 8- and 32-layer panels, for which the average was calculated for three pieces).

Depending on the results of ballistic tests, the technology may be improved for the selected thicknesses, in order to reduce the time of manufacturing and control, based on the experience gain in making these sets of panels.

Table 4.6. Characteristics of the elaborated panels

Panel type	**Average thickness**	**Standard deviation**	**Panel mass**	**Surface density**	**Fiber / panel mass ratio**
	[mm]		[g]	[kg/ m^2]	
OGe8	6.37	0.029	1116	12.39	0.747
OGe16	12.49	0.427	2221	18.59	0.752
OGe20	15.53	0.550	2821	22.97	0.733
OGe22	18.11	0.940	3196	25.15	0.709
OGe24	18.26	0.225	3183	27.51	0.778
OGe32	25.73	0.857	4506	36.55	0.729

Chapter 5. Experimental Campaign and Evaluation of Results

5.1. Ballistic Protection Standardization

Standardization in the field of ballistic protection, more than in other areas, is in line with the principle of CEN/CENELEC statement that "standards build trust" [76] and promotes innovation and introduction of new high-performance solutions, based on test procedures to promote the use of new, high-performance solutions, that are able to demonstrate quality and safety for such systems. In recent decades, testing methods have been refined and measuring devices have become more complex [11], [53].

The standard specifications are used for:

- evaluation of performance and quality by tests,
- evaluation of new or improved materials and solutions, under the same conditions as for “classic” ones,
- investigation and understanding of the failure mechanisms of protection systems,
- logical, integrated approach to ballistic threat protection solutions,
- understanding and avoiding the consequences of hits on personnel and equipment,
- protection and maintenance of the availability of staff and equipment at an effective level.

Ballistic protection tests are performed under imposed and customized conditions. In reality, the conditions may be different. A test condition is assessed as sensitive if a relatively minor change is sufficient to produce a much different result [37].

Regulations may be grouped into two classes:

- standard recommendations included in national or regional legislation; they are developed by organizations recognized as having as main mission the standardization and become mandatory,
- recommendations that are not included in the legislation; these are instructions established by economic or public organizations in order to be able to have a reference testing system for certain products.

Test methods have two variants, both of which are applied to these products:

- testing of a defined minimum penetration velocity (V_{50}), which provides information on ballistic protection, while revealing product quality and production options for the protection system,

- test at a defined impact velocity, for which the protection system is not fully penetrated and with a sufficient safety factor for a required number of hits.

Table 5.1. Information from a ballistic test report

– Information about the contractor	– Test personnel and any witnesses agreed by both parties
– Measuring and recording equipment	– Used weapon or weapons
– Information for contacting the test staff / company	– Information on used projectiles: code, mass, construction solution or variant, materials, dimensions, supplier, design, conditioning
– Lot number and quantities	– Information on propulsion material: type, mass per stroke, composition etc.,
– Specifications for the tested issue and its code/number	– The results include: the impact velocity in the calculation for V_{50}, with the highest (deepest) partial penetration, the lowest value for complete penetration, spreading intervals of the test parameters, and the results
– Specifications for the tested product	– Characteristics of the witness panel / system
– Armor material description	– Notes on how to perform the test or on the behavior of the material / system
– Identification of the material for each sample	– Photographs, films, images obtained under a microscope or by other means agreed by interested parties
– Temperature and humidity in the test facilities	– (If required) the mechanisms of failure to be highlighted
– Date of tests	– Standard or regulation number

Table 5.1 shows the information included in a ballistic test report. The results are compared, qualitatively and quantitatively (by parameters and measurements) to the requirements of the standard, if the interested parties request so. For equipment protection systems, some aspects related to

standardized or non-standardized ballistic protection tests are given in Fig. 5.1.

In standards, threats are classified into levels and, as a result, a system provides protection against threats of a certain level. It is not allowed for assuming that a higher level recommends the product to be used at a lower level without testing.

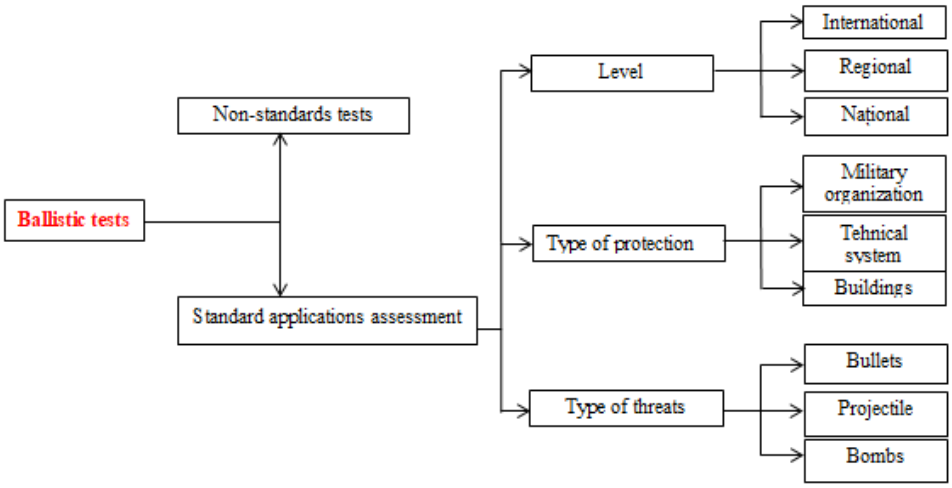


Fig. 5.1. Tests for ballistic protection

New hybrid composites are currently entering this particular market because they have improved parameters in terms of strength-specific density ratio, longer life and better thermal properties [56].

The advantages of using non-standard samples (as dimensions) are:

- availability to be fabricated out in the laboratory (usually 100 mm to 250 mm square samples are made),
- easier to attach to laboratory frames,
- easier to carry out further investigations with the help of fast film cameras, thermal cameras etc.,
- easier to cut samples to be analyzed using scanning electron microscopes, laser profilometers or atomic microscopes, etc.

Disadvantages of using non-standard samples may include:

- difficulty in extrapolating the panel response when it is larger; in this field of ballistic protection materials such extrapolations are only accepted at the design level, a trend which must be verified by tests,

- small sample sizes may show some failures, but may screen others or even prevent the development of some, such as delamination,

- the fixing mode may induce a different response as compared to the actual panel, which may be mounted in a more complex frame (e.g. vehicle doors).

Standardized test procedures are usually applied after preliminary laboratory-scale tests that meet only a few of the requirements of the standard, in particular those required by the nature and type of threat (type of projectile and its velocity and mass). At first, the technology of making the samples depends on their size and, thus, the response of the non-standard sample may differ from that obtained on the standard panel. Also, the actual solution for implementing ballistic protection may differ, including the shielding system, the presence of other components of the system to be protected, and may influence performance (such as the edges or corners of ballistic protection panels).

5.2. Test Campaigns for Rigid Panels (Shields or Shield Components)

Glass fiber composites may have satisfactory results, but it is not recommended for very high velocities or for protecting the human body [1].

The objective of this chapter includes:

- testing whether the packages developed by the author withstand the ballistic impact with a 9 mm FMJ bullet, according to Ps-02512C-14.00-017 Determination of resistance to the impact of projectiles, SR EN 1523-l: 2004 [78].
- investigating the processes and stages of failure using macro photography, SEM images and elemental analysis (EDX),
- establishing the influence of the number of layers for the designed panels, based on the experimental results.

For this research study, the tests were performed on panels made of the same materials, but with a different number of layers of quadriaxial fiberglass fabric: with 8 layers and 32 layers (3 panels available) and with 16 layers, 20 layers, 22 layers and 24 layers - (5 panels available for each number of layers).

5.3. Test Equipment

The test campaign aimed to evaluate the behavior of ballistic protection panels made by the author, at the action of bullets of 9 mm FMJ caliber, by firing in a specialized laboratory, the method being the one recommended in the standard EN 1522/2004 [77].

The velocity of impact is denoted by v_0 and is measured using a projectile velocity measuring system, the Őehler 43 chronograph. The chronograph makes the following measurements: velocity at the mouth of the barrel, projectile time in the air, velocity at the target. A scheme of arranging a firing laboratory is given in Fig. 5.2.

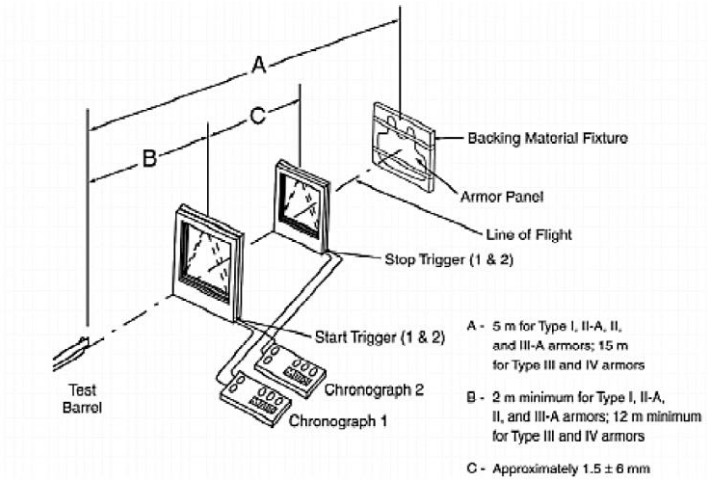


Fig. 5.2. Monitoring and measuring equipment for tests [81]

5.4. Test Methodology

The determination of the ballistic resistance of the ballistic protection panels to the action of the 9 mm FMJ caliber infantry bullets was performed according to EN 1522/2004, as follows: the bullet hits the target with an average initial velocity of 373 m/s, from a distance of 5 m (normal conditions), except for the dimensions of test pieces, which were 300 mm x 300 mm, as compared to 500 mm x 500 mm as required by the standard. The laboratory press, the available material, the oven available for the heat treatment of the composite allowed only these dimensions, 300 mm x 300 mm.

The fires took place in the laboratory of the Center for Research and Innovation for Defense CBRNE and Ecology, Bucharest, and were carried out by qualified CCSACBRNE personnel. The tests were performed

according to the operating procedures and working instructions approved by this laboratory. The rules of protection and regulations specific to this type of laboratory have been observed.

All panels were made according to the laboratory-scale technology, designed by the author (see Chapter 4).

Environmental conditions in the laboratory were: temperature: 21 °C ± 5 °C, relative humidity: 65%, atmospheric pressure: 764 ± 15 mm Hg.

The following steps are required to perform the test:

- the test equipment is positioned in the mounting frame, at the required distance from the mouth of the fire barrel; the types of weapons and ammunition are for the level FB2 [77].

- position the bullet velocity measuring system, with a distance of 2 m from the mouth of the barrel, so that the frames of the system are in planes perpendicular to the firing direction; the distance between the frames of the velocity measuring system is 0.5 m; the distances are measured with an accuracy of 1 mm;

- 3 shots are fired on the test panel, these being arranged in an equilateral triangle, with a side of approximately 120 mm.

5.5. Results Obtained from the Performed Tests

The obtained results and the mechanisms of target failure (at full and partial penetrations) are further discussed in order to improve the response of the target, by changing parameters, such as the number of layers of the panel.

For 12 measurements of projectile velocity, the results are given in Fig. 5.3, the average velocity being 372.66 m/s, with a standard deviation of 2.211 m/s, which represents only 0.59% of the average velocity, maximum value being 376 m/s, and the minimum one 369 m/s. The average velocity, with which the tests were performed, corresponds at least to the FB2 level of protection, being intermediate between the FB2 and FB3 level.

Front and back photos of the panels were taken. The face was considered the surface of the composite that first comes in contact with the projectile and the back the opposite side of the composite. In addition, one of the plates was cut with high-speed abrasive disk to be able to reveal the projectile's orifice.

This summary presents results for 8-layer, 16-layer, and 24-layer panels, but the test campaign also included 20-, 22-, and 32-layer panels.

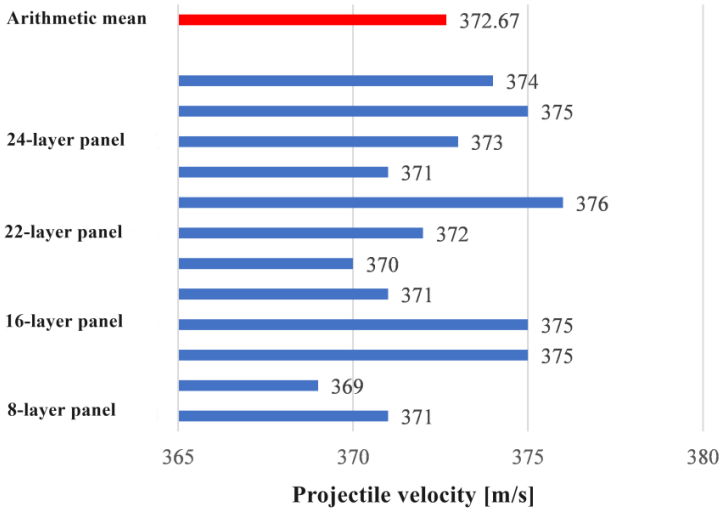
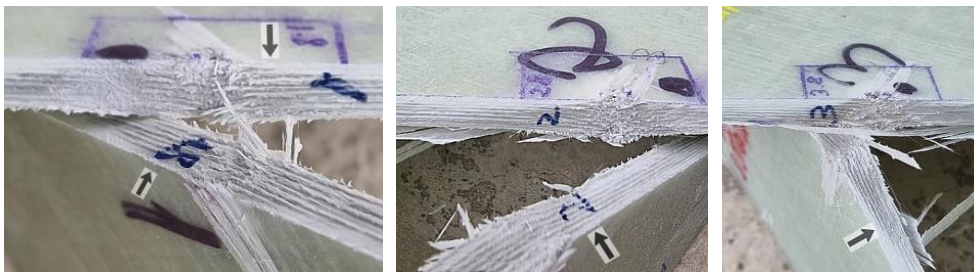


Fig. 5.3. Projectile velocities (measured for each fire)

Figure 5.4 shows the details of cross sections through the 8-layer OGe8 panel. A total penetration is observed, the three fires produce a similar destruction to the panel, not noticing an increase in the damage of the orifice, depending on the order of fires, which means a good qualitative response of the panel to multiple impact. There is a slight delamination of the sublayers on layer 1 and the sublayers on the last layer of this composite panel. On the faces of the panels, the delamination is influenced by the direction of the yarns on these surfaces. There is delamination also between the intermediate layers, the size of the delaminated surfaces being more visible in view of the back surface of the panel(Fig 5.5). The front of the panel is considered to be the surface that is impacted by the projectile and the back of the panel is considered the surface opposite to the projectile impact.

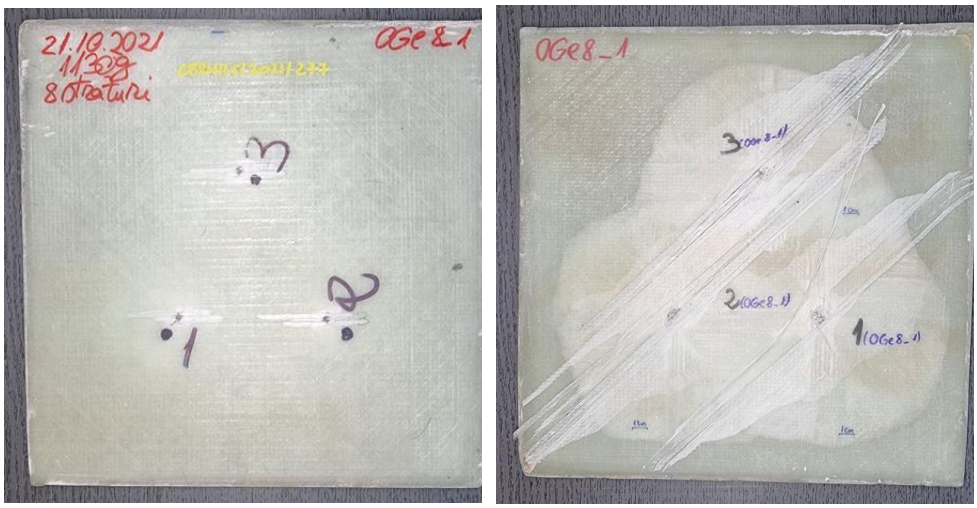


a) Fire 1 b) Fire 2 c) Fire 3

Fig. 5.4. Ballistic protection panel OGe8 (dry cut with high speed disk)

The fact that delamination is more visible as a color difference on the back view shows that this process is more intense in the last layers. The almost circular shape of the delamination for each fire indicates that the architecture of the fabric (0°/45°/90°/-45°) makes almost uniform the behavior of the panel with layers with quadriaxial orientation of the yarns.

Delamination on the face layer 1 is localized and depended on the positioning of the yarns on the first sub-layer. On the panel back, the delamination can be seen in the thickness of the plate by a change in color. Circles with close size diameter are observed, the areas overlapping the circular delamination areas, not suggesting further damage. On the back, the last layer is more destroyed, clearly observing the -45° orientation of the yarns on the last sub-layer. The quality of the response to multiple hits is observed by the small differences between the dimensions of the delaminated areas for each fire, but this difference is quite small.



a) b)

Fig. 5.5. The 8-layer panel after being tested, a) front, b) back

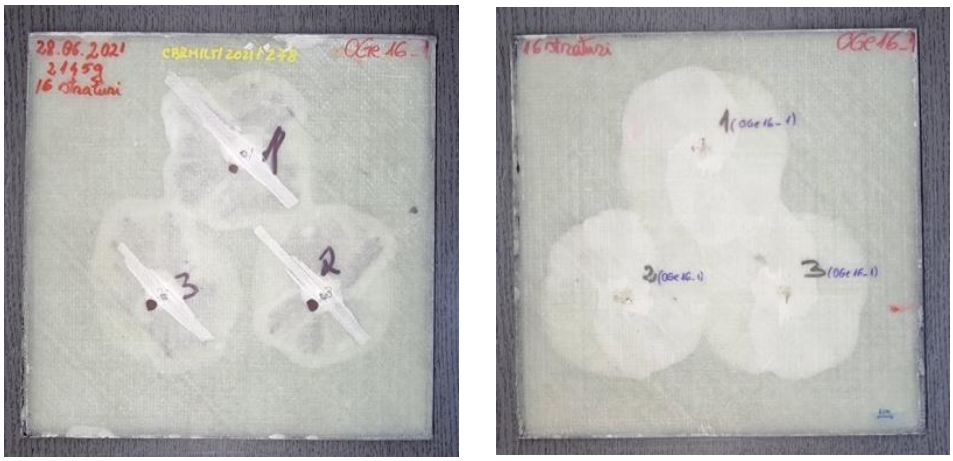
The delamination looks different on the front of the panel than the delamination seen on the back of the panel. The delamination on the face of the first layer highlights the orientation of the yarns on the first substrate of layer 1 (here 0° orientation) and on the back of the panel the orientation of the surface sub-layer at -45° is evident, with a more intense delamination.

From all the photos of the back surfaces of panels, it was observed that this quadriaxial fabric generated traces of almost circular delamination, and their diameters have close values, which qualitatively reflects a behavior of the layers without a pronounced anisotropy in the panel.



a) Fire 1 b) Fire 2 c) Fire 3

Fig 5.6. Ballistic protection panel OGe16 after being tested (the panel with 16 layers of quadriaxial fabric)



a) b)



c)

Fig 5.7. Results of fires on 16-layer panel after being tested: a) face, b) back, c) cross section through two fire orifce

Figure 5.6 shows the details of the cross sections through the 16-layer OGe16 panel. For this panel, the penetration is partial, within 2-3 layers. For this threat, defined by the size, materials and speed of the projectile, the 16-layer panel resists very well, although traces of delamination are visible on the front and the back of the panel. From these sections, there is a strong delamination between the last perforated layer by the projectile and the layer on which it stops. The outline of these large delamination can be seen both on the front of the panel and on the back. The delamination on the back is quite advanced.

A cross section through two fire orifices, fires 1 and 2, (Fig. 5.7c), shows a similar damage for both hits, the distance between the fire points did not lead to a continuous detachment in the delaminated area, a very fine delamination is observed (very small spacing between layers) for the last layers, visible by the color change on the back of the panel.

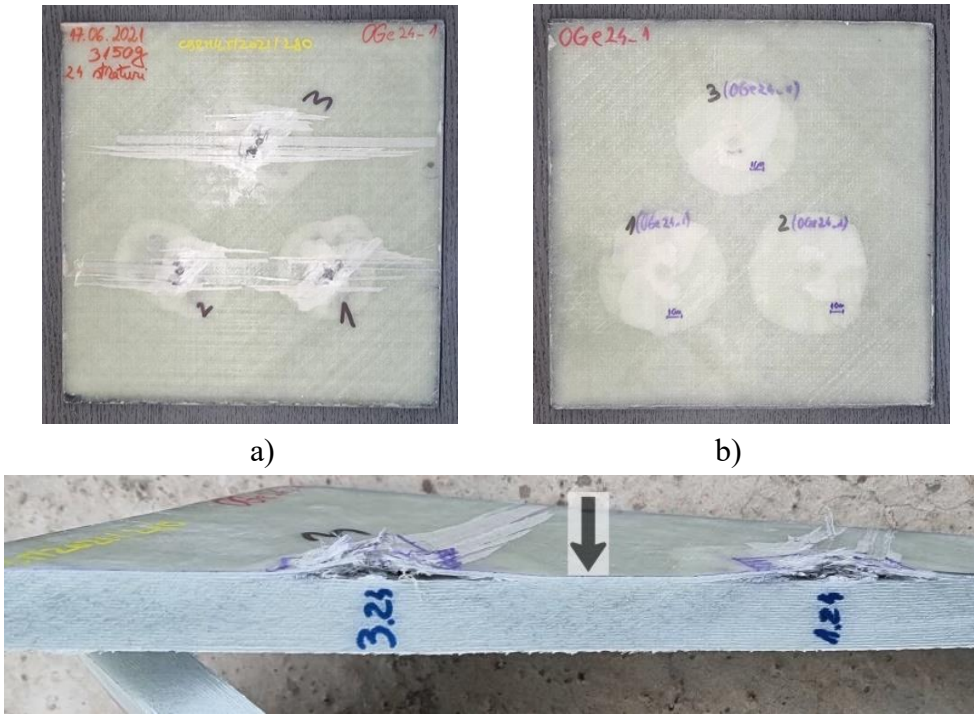
The delamination has an almost circular shape, which reflects the fact that the quadriaxial fabric induces a quasi uniform response in the plane of the fabric. On the back of the panel, even in the direction of impact, shallow cracks are observed, implicitly a few broken yarns can be seen on the macro photographs, although the area between the layer on which the bullet stopped and the back of the panel is not cracked in the direction of impact (Fig. 5.7).



a) Fire 1 b) Fire 2 c) Fire 3

Fig 5.8. Ballistic protection panel Oge24, after being tested

Figures 5.8 and 5.9 show details of the cross sections through the OGe24 panel, with 24 layers of quadriaxial fabric. For this panel, the penetration is partial, only 2-3 layers being broken. The 24-layer panel resists very well. From these macro-photos, no large deformations of the last layers are observed, highlighting the rigid character of the panel, for this threat.



a) b)

c)

Fig. 5.9. Results of fires on 24-layer panel, after being tested: a) face, b) back, c) cross section through two fire orifce

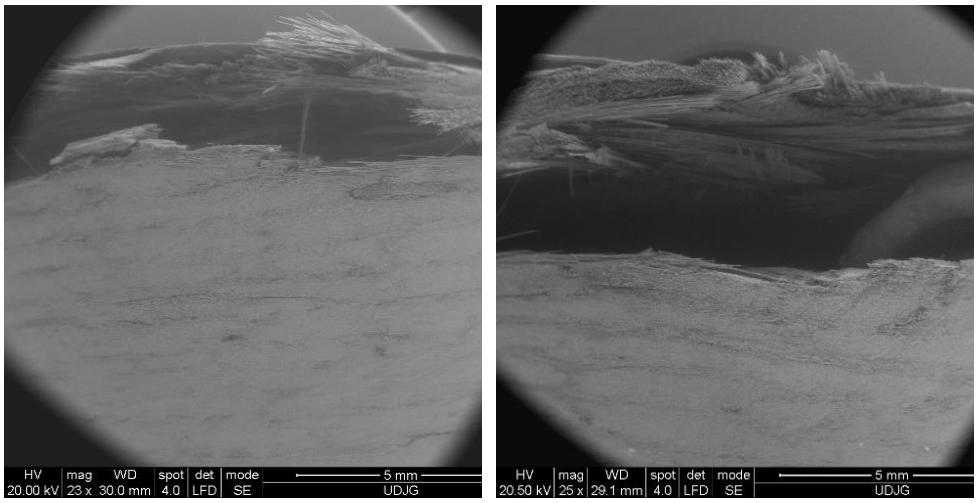
5.6. Failure Mechanisms in Tested Composites

Given the nature of the materials possible to be highlighted under the microscope (metals, polymers, glass fibers), the samples were coated with gold. Prior to analysis under an electron scanning microscope, the samples were mounted on an aluminum support by fixing with double-sided adhesive carbon tape. Due to the poor conductance of polymers or polymer-containing composites, it is necessary to cover (metallize) the sample surfaces by a process of vacuum spraying (sputtering). This process consists of applying a very thin layer of gold (maximum thickness 7 nm), and the used equipment was the SPI Sputter Coater Module (SPI Supplies, USA). Plasma discharges with a current intensity of 18 mA occur in a controlled atmosphere with atoms of an inert gas (argon). Working conditions were: maximum coating time 120 s, vacuum pressure 0.1 mbar.

Depending on the tested level, the type of projectile and the nature of the target materials, there may be two situations:

- when the thermal effects of the impact may be negligible,

- when the thermal effects of the impact are not negligible [4], [5], [65].



a) 16-layer panel b) 20-layer panel, fire 1

Fig. 5.10. Delamination between the layer that stopped the bullet and the last layer that was broken (penetrated)

Figure 5.11 synthetically presents mechanisms of target failure. Although they can be described separately, on the target, on the penetration hole, on the destroyed layers or near them, these mechanisms can overlap, the result being synergic and, sometimes, more difficult to identify.

These failure mechanisms should be differentiated according to the impact resistance of the target:

- mechanisms characterizing total penetration and
- mechanisms characteristic of projectile arrest.

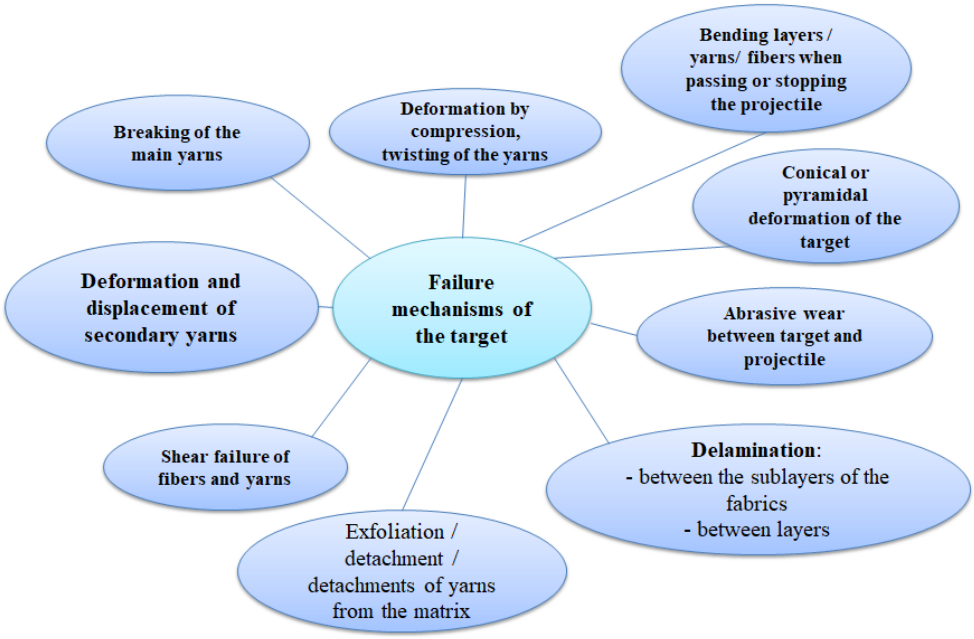


Fig. 5.11. Failure mechanisms of the hit composite target

For the panels in the second category, the particularities and the intensity of the processes are also dependent on the thickness of the target.

Delamination may occur between layers and/or between sublayers. The shape, size and area, where the delamination occurs, may differ depending on several factors, including the type of penetration (total or partial), the panel thickness and the characteristics of the threat (projectile type, impact energy, materials included in the projectile).

The total penetration makes visible several areas of delamination, more intense between the first and last layers. The absence of a material in front of the first layer or behind the last layers initiates delamination and develops it, substantially.

Three areas with delamination may appear at partial penetration:

- between the first layers, the mechanism and aspect of delamination being close to those of total penetration; the first layer has curved yarns, with a curvature outside the initial plane of the layer,

- intense delamination between the last perforated layer and the first layer on which the projectile stops, as stopping the bullet forces it to deform

laterally and to fragment, the fragments being pushed sideways, forcing delamination,

- delamination between the last layers, more visible on thinner panels with partial penetration (16 layers) and less on thicker panels (with 24 layers and 32 layers).

It is observed that the passage of the projectile is not well delimited due to the asymmetric rupture of the successive layers of fabric (and due to the orientation in various directions of the yarns from the 4 sublayers of the fabric. Details for the penetration hole, from which the different orientations of the yarns on different substrates of the fabric can be observed, are given in Fig. 5.12.

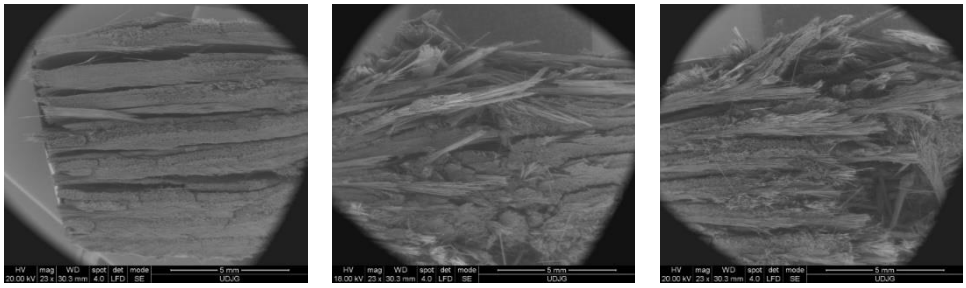
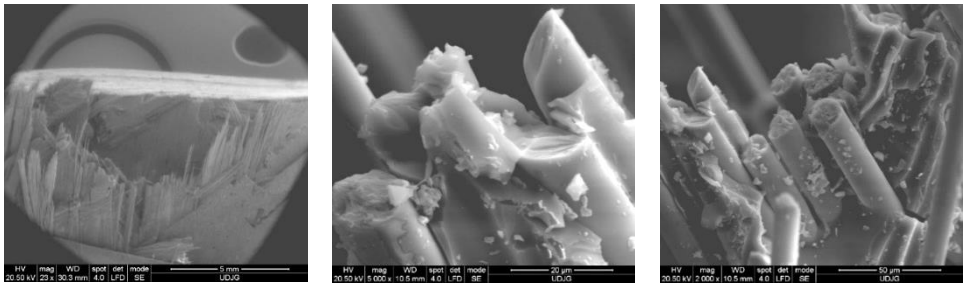


Fig. 5.12. SEM images, in the cross section of the 8-layer panels (total penetration)

Figure 5.13 presents a top view of an almost circular rupture (orifice), a few fragments of yarn or layers are pressed on the first layer that resisted and which, in turn, cause the bullet to fragment in many pieces and push them laterally, opening more the already delaminated layers. Figure 5.13a shows a detail of fire 1 on the 20-layer panel.



a) View of the orifice b) Detail from c) c) Detail from a)

Fig. 5.13. Details of the 20-layer panel, fire 1

5.7. Identification of the Components that Participated in the Impact, by EDX Analysis

Figure 5.14 shows an analysis of the chemical elements of a current area in the cross section of the 22-layer composite (OGe22), after testing, for fire 1.

The image is taken in the direction of impact, through the bullet hole. It is observed that the light-colored material is the Lead-Zinc alloy, from which the projectile core is made of, and the printing of the fabric on the Lead alloy, hence traces of carbon (from the composite resin) and Aluminum, Oxygen (from the oxides included in glass fibers). Traces of metallic elements (Sn, Sb) may be from the jacket alloy, and other metallic elements, such as Zn, may be left from the core. Copper is present in this spot area as a result of the friction of the Lead alloy with the jacket, during the compression of the core in the cavity generated by the lateral pushing of the bullet, when it was stopped.

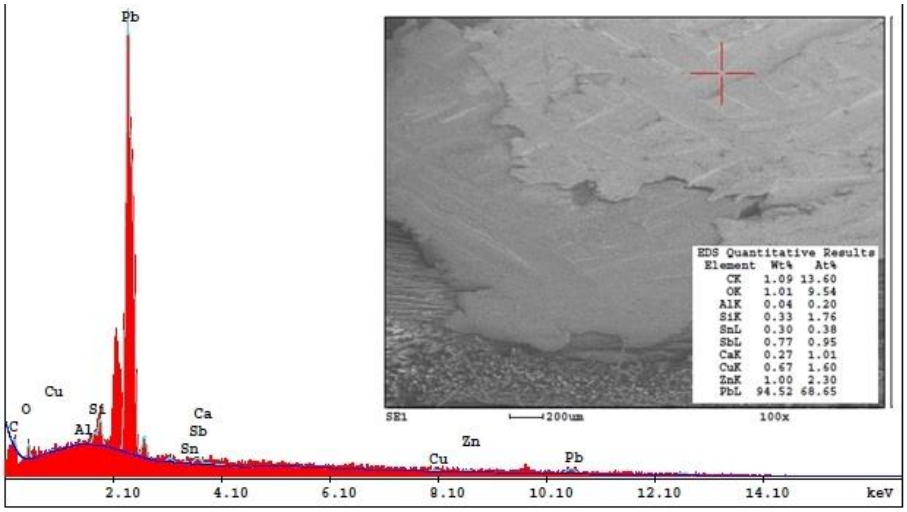


Fig. 5.14. EDX elemental analysis, detail from 22-layer panel, fire 1

On the SEM image in Fig. 5.15, a rectangle with red lines was outlined to identify where the lighter colored material came from. The analyzed area contains a lot of Pb (64.79% wt), which means that the lighter fragments are from the core of the projectile. The presence of quite high carbon

concentration (27.19% wt) shows that relatively small matrix fragments, of the order of tens of microns at most were mixed in the mass of the core, due to the impact.

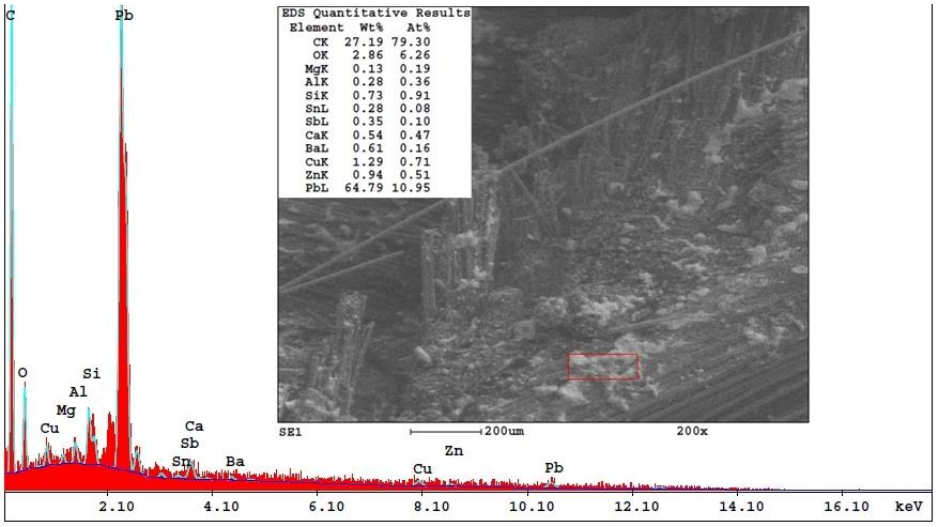


Fig. 5.15. Fragmentation and spread of the lead core of the projectile (panels of 24 layers)

Figure 5.16 shows a detail of the impact area on the layer where the projectile stopped, highlighting the following: broken fragments of the matrix, fragment of fiber (top left corner), spheroidal fragments from projectile core. These were analyzed by EDX, proving that the noticed micro-drops (which are rare) are made of lead alloy, the shape suggesting that, due to the impact velocity (373 m/s), small pieces of lead alloy ended up in a molten state and they rapidly solidified. The Lead concentration in this point area is 81.45% wt, the characteristic elements of the fiber not being present, but possibly even smaller fragments of the matrix to be included in the lead alloy drop, because the local concentration of C is 12.37% wt.

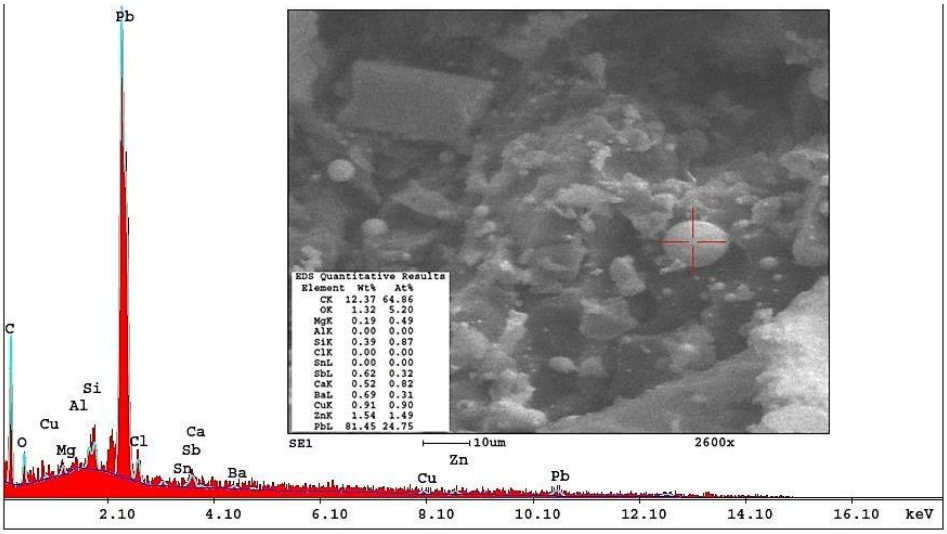


Fig. 5.16. Melting and solification of fragments resulted from the projectile core (24-layer panel; view through the orifice)

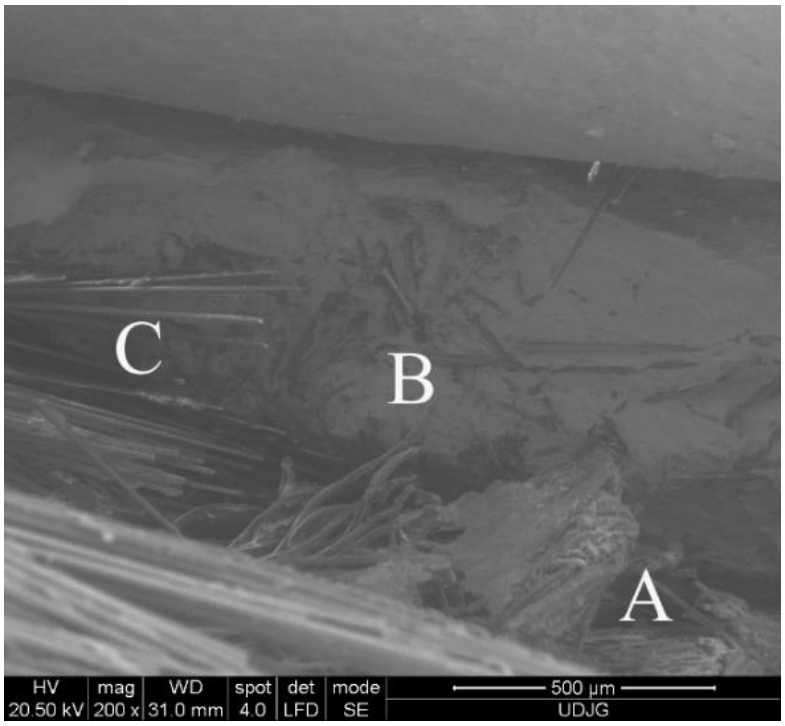


Fig. 5.17. Failure mechanisms in the zone where the bullet was arrested, panels of 16 layers

Figure 5.17 presents failure mechanisms in the area where the projectile was stopped, A - composite fragment, detached from the destroyed layers and crushed on the layers that did not failed; B - the core of the projectile, strongly deformed and with fragments of glass fibers; C - broken yarn, made of fibers, from which the matrix had been detached.

5.8. Conclusions on the Ballistic Impact Behavior of the Designed Panels

After performing the tests (which were classified at FB2 level) and comparing the results by the number of broken layers on the hit panels, the following were found: the 8-layer panel was completely penetrated, the other panels withstood partial penetration with the destruction of several layers (16-, 20-, 22-, 24- layer panels had 3-4 broken layers each, and 2 layers were broken on the 32-layer panel and, for these panels, the bullet was bounced).

The increase in the thickness of the tested panels led to a reduction in the circles that suggest delamination on the panels' back, reflecting the fact that the delamination phenomenon decreases in intensity (towards the back of the panels) if the number of layers in the composite increases.

The following conclusions can be drawn from these results.

For the tested level, the 16-layer panel is sufficiently strong, the reduction in the number of layers can only be discussed after performing tests on panels with intermediate thicknesses (between 8 layers and 16 layers).

Given the behavior of thicker panels, of 20 to 32 layers, the author proposes to continue testing these panels for a higher level, level FB3 and FB4, according to SR EN 1522: 2004.

The analysis of macro photos and SEM images highlighted the failure processes of the composite and the fact that the selected materials (fabrics and resin) are suitable for this application.

Chapter 6. Conclusions and Personal Contributions

6.1. The Importance of the Theme

The doctoral thesis entitled "A Theoretical and Experimental Study of Ballistic Protection Packages Made of Glass Fibers" is part of the research on ballistic protection of equipment. „Modern war is becoming less and less a direct confrontation between two armies of states or alliances, and more and more a confrontation between two economically and militarily disproportionate forces, in which each side tries to find new techniques to win the battle" [59].

The aim of this doctoral thesis was to design, at laboratory scale, and to characterize a protection composite panel, based on unidirectional quadriaxial glass fiber fabric in epoxy matrix, by the help of a numerical analysis and a test campaign. A macro-scale model was validated and could be applied to improve the initial solution and reduce the intervals of parameters, such as the number of layers. The test campaign tracked the behavior of ballistic protection panels, under the action of the 9 mm FMJ bullet (FB2 level, the average impact velocity being 373 m/s).

6.2. Final Conclusions on the Ballistic Resistance of the Tested panels

This research study is a unitary work and includes a documentary synthesis on the results reported in the open literature, on reported experiments for ballistic performance of materials and protective panels made of glass fiber fabrics, done with the help of database access, offered by the Library of "Dunarea de Jos" University. The document has 6 interdependent chapters, which, in succession, provide solutions for interpreting and understanding the behavior of layered composites, with multiaxial glass fiber fabrics, based on data obtained by simulation and testing.

Chapter 1 highlights recent studies (reports, doctoral theses, books and articles published in prestigious journals) on testing ballistic panels, with reference to those made of glass fiber fabrics. This documentation is the starting point, from which the development of the research was initiated, and makes a review for the research on ballistic protection panels, at international and national level. Ballistic protection systems exist in a wide variety of solutions, in terms of their structure, as well as the nature of involved

materials and their combinations. The diversity of interactions and failure mechanisms in the behavior of impacted materials require a systematic approach to the design of ballistic protection and a detailed analysis of failure. Analytical models, empirical or semi-empirical ones, try to describe the behavior of the protection system in particular cases, with applicability in a narrow range of parameters of influence, often for only for a particular threat.

Chapter 2 presents a logical scheme of this research study, suggesting the connections among chapters and activities performed by the author. The diagram emphasizes the connection between the simulation and the experimental results and the importance of this connection in improving the final design solution of the ballistic protection panel.

Chapter 3 presents an impact simulation using a parametric model, at macro level. The parameters considered by the author were: the impact velocity of the projectile, the number of layers of the modeled panel. The model introduced constitutive material models that take into account the strain rate, for the core and jacket of the projectile. Delamination was modeled from a jump (initiation) condition of the crack when certain values of the tensile and shear stress are reached. The model introduced a failure criterion based on equivalent plastic strain (EPS), by characteristic values for each of the materials that participated in the impact.

By simulating the impact bullet-layered panel and studying the influence of panel thickness (for panels of 8-layers, 10-layers, 12-layers, 16-layers and 24-layers), the total penetration for the 8-layer panel and the partial penetration for the other panels were highlighted. From the results of tests presented in Chapter 5, all 8-layer panels had total penetration, without retaining the bullet. From the simulation of impact process on the 8-layer panel, a failure of the panel with total penetration was obtained, as in the case of laboratory tests. For the other panels (16- to 24-layer panels), a validation of the model developed by the author included the number of broken layers in the simulation, this being the same as the number of broken layers obtained from the experimental tests.

For the thicker panels, of 16 layers, 24 layers, experimentally, 3...4 destroyed layers were obtained, as they were obtained on the layered panel model. The actual layer of quadriaxial fabric was modeled in a simplified manner, as being an isotropic material, a simplification argued by the fact that the arrangement of unidirectional yarns at (0°/45°/90°/-45°), has the tendency to make uniform the mechanical properties of the layer in plan. The

mechanical properties of glass fibers were taken from the specialized literature [50] and from the product catalog of Castro Composites SL. In the simulation, the destruction of the bullet is similar to that observed in experiments for the actual projectiles that totally or partially penetrated different panel variants, but the deformation and fragmentation of the bullet in the simulation is not as severe as that resulting from laboratory tests. This could be the results of used software (Ansys Explicit Dynamics) that did not take into account the thermal effect on the materials.

The model for the impact projectile-panel, designed and run by the author, in Ansys Explicit Dynamics, has a macro level, with the following features:

- all bodies and materials involved are in the elasto-plastic field, with EPS failure criterion (equivalent plastic strain at break); many references studied by the author, have one of the bodies (the projectile, most often) considered rigid [16] [44], which changes the response to impact, substantially,

- the delamination was modeled from the condition of the separation of bonds between layers, when a value of the tensile and shear stress is reached, a model that gave satisfactory results regarding the size of delamination between the layers, as compared to the experimentally obtained delamination,

- stages for full and partial penetration have been identified on simulated cases;

- simulations were performed for the tested panels (as dimensions and layer structure) and the model was validated based on the number of broken layers (± 1 layer) and the size of the delamination on the back of the panel,

- cases were simulated for intermediate thicknesses between 8- and 16-layer panels because, from the results of the laboratory tests, a “reserve” of impact resistance was found, in the sense of establishing, at the modeling level, effective thicknesses, but smaller, for the same threat,

- only for this study, in total, 5 cases were run at a speed of 375 m/s, velocity that was near the average velocity of tests performed in the laboratory (373 m/s) and 3 cases for the impact velocity of 420 m/s, characteristic for a higher level of protection (FB3), with the same ammunition.

From results obtained for these runs, the following conclusions could be drawn:

- although the layer material model was simplified to an isotropic bilinear model with hardening, based on literature data, the results obtained

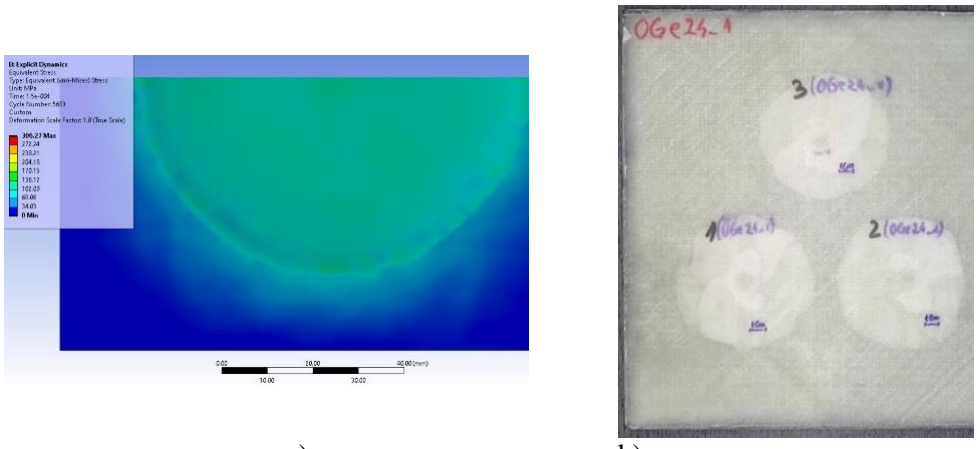
for the parameters, with which actual tests were performed, were validated by the number of layers destroyed for the partially penetrating panels, and by the delamination size on the back of the last layer,

- analyzing equivalent stresses (values and distributions), at different time moments and in different layers, it was possible to distinguish the impact stages for total and partial penetration,

- based on the results for the tested panels, cases with intermediate thicknesses (or number of layers) were run between 8-layer panel and 16-layer panel; simulations were run for 10- and 12-layer panels that resulted in a numerical solution that could be validated by laboratory testing and could provide good ballistic protection, but with lower surface density (and, implicitly, panel thickness).

The same model was run for specific conditions of level FB3, for thicknesses of 8 layers, 16 layers and 24 layers, which showed that the last panel could withstand the next level of protection very well, with the same projectile, but of higher velocity (420 m/s).

Figure 6.1 shows an example of comparing the delamination size on the last layer (panel back) in simulation and the experiment, for the 24-layer panel. The difference between the delamination diameters was only 13 mm, which represents 12.9% of the experimentally obtained delamination diameter. Similar or smaller differences were obtained for other thicknesses (for partial penetration).



a) b)

Fig. 6.1. Delamination, view on the panel back for the 24-layer panel: a) from simulation (87.60 mm), b) on the back of the tested panel (100.60 mm). Testing conditions: impact velocity of 375 m/s

Running simulations, by the help of the finite element method, as close to reality as possible, for higher impact velocities, are conditioned by aspects related to large displacements and strains, cracks, methods of erosion of too small or/and too deformed elements etc., nonlinearities of the behavior for materials involved and their properties at high strain rates. The use of Explicit Dynamics solver, specialized in simulating dynamic processes, with the introduction of complex material models, based on experimental results, helps to significantly reduce test intervals for certain parameters, such as panel thickness (number of layers), sequence of materials in hybrid panels, layer assembly. The simulation is very useful because it reduces the costs related to produce the first samples and the tests.

The designer of a ballistic protection system may significantly reduce time, human and financial resources involved in experiments by analyzing data experimentally obtained with those resulting from numerical simulation, in order to optimize.

Chapter 4 presents a laboratory-scale technology, through which panels of various thicknesses may be obtained by brush laying-up, pressing and heat treatment. The process applied by the author has repeatability, precision and robustness. The recipe for producing this panels and the laboratory-scale technology are original. The fabrication was made in compliance with the norms of safety and health, with adequate protective equipment. Ballistic protection panels (coded OGe) are intended for light shielding for vehicles and protected enclosures and ensure the degree of survival in protection actions for the specified level (FB2, according to EN 1522/2004 "Windows, doors, shutters and blinds. Bullet resistance "Conditions and classification" and SR EN 1523/2004 "Windows, doors, shutters and blinds. Bullet resistance. Test method"). The author used a high-strength quadriaxial glass fiber fabric, 1200 g/m^2, (0º/+45º/90º/-45º), also for ballistic applications, and two-component epoxy resin (BIRESIN CR82 with Biresin hardener CH80-2), with heat stabilization treatment.

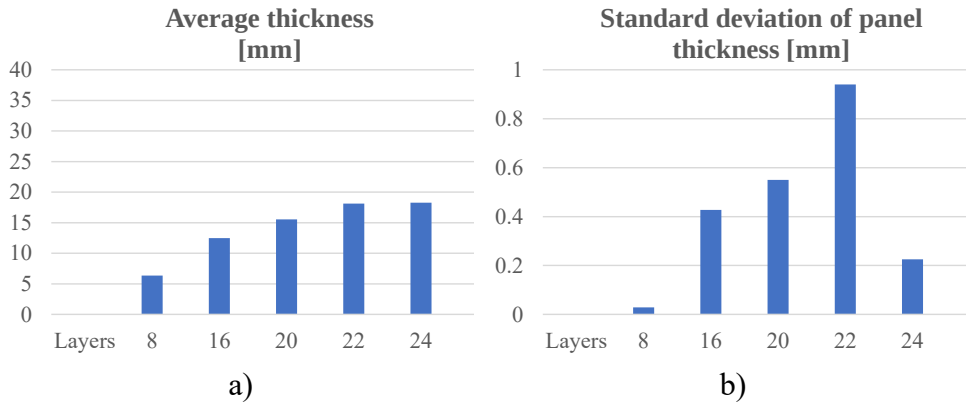
The technological process for obtaining OGe panels, of various thicknesses, includes a succession of phases: cutting the fabric layers (and weighing the set of layers that participates in making the panel), making the resin + hardener mixture, brush laying-up and pressing, panel thickness monitoring in press, a natural aging of 7 days and a final control, a heat treatment at 60 °C, for 6 h and a quality control (weighing, thickness measurement, calculation of standard deviation and surface density).

Analyzing the values of panel characteristics (Fig. 6.2), it was noticed small standard deviations and an almost constant mass ratio for glass fiber/panel, regardless of the panel thickness (the average values are for 5 panels in a set, except for 8-layer and 32-layer panels), which had only 3 samples.

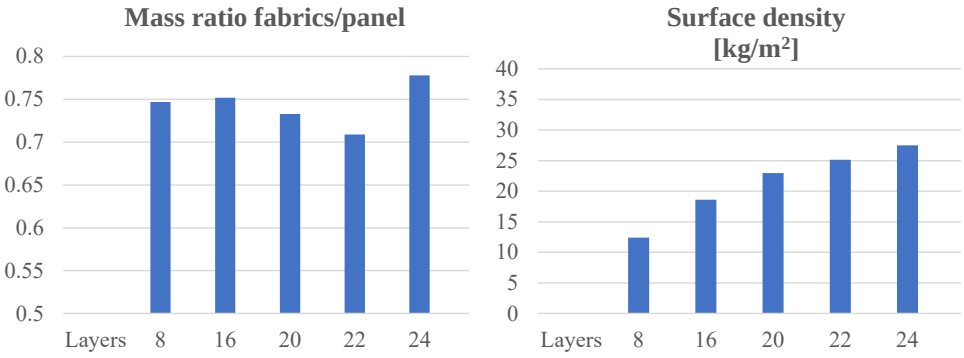
Chapter 5 presents the results of the tests performed in the specialized laboratory of CCIACBRNE, Bucharest, the measuring and monitoring equipment, the test procedure, standards applied in this test campaign. The results of ballistic tests, accompanied by research report, were analyzed using photographic and SEM images, justify their recommendation to be used in prototypes of protection systems. Based on SEM images, EDX analyses and macro-level photo sets, the author described the failure mechanisms, characteristic for this type of ballistic protection panel (layers of quadriaxial glass fiber fabrics and epoxy resin).

For the measured impact velocity (373 m/s ± 3 m/s), the projectile was stopped after the integrity of first layers was destroyed (2...4 layers for 16-layer, 20-layer, 22-layer and 24-layer panels), which reflects a lower dependence on the penetration depth of projectile in the case of the composite with a higher number of layers. For the 32-layer panel, the failure of a number of 1…2 layers was noticed, with the rebound of the severely fragmented projectile.

Chapter 6 presents the importance of the research, final conclusions based on numerical and experimental results, the author's contributions and future research directions in the field of using composites in ballistic protection systems.



a) b)



c) d)

Fig. 6.2. Characteristics of the produced panels

6.3. Personal Contributions

The results of the research study and the synergistic approach between experiment and simulation led to highlight the following original contributions in designing and testing ballistic protection materials:

- selection and critical analysis of the documentation related to materials, tests and modeling of fabrics and panels with ballistic applications,
- identification and justification of the research objective in using glass fiber composites,
- design of a numerical model of the impact projectile-layered panel, at macro level, to assess, by simulation, the impact resistance of a family of panels.

The model was run to highlight the influence of the number of layers and the influence of the impact velocity of the same projectile, up to FB3 level. The simulation results were validated by laboratory tests for 8-layer, 16-layer, and 24-layer panels, taking into account the following validation criteria: the number of destroyed layers and the size of the delamination visible on the last layers. The simulation was used to detail the impact response of the panels with a number of intermediate layers, between 8 layers and 16 layers, because, from experimental data, it was found that the 16-layer panel withstood very well (FB2 level) and, therefore, a study on the model may recommend a thinner panel that can withstand the same threat. From data obtained from simulation, preliminary laboratory tests on the 12-layer panel may be recommended. The simulations were also performed at higher velocity (420 m/s, corresponding to FB3 level), because, from the analysis of the panels' failure, at FB2 level, it may be recommended to test panels of 12-

and 16 layers for a higher level. It should be emphasized once again that for this high-risk domain of ballistic protection, the extrapolation of simulation results should be done only on the basis of subsequent laboratory testing, analysis of the test campaign results consisted of panel recommendation for FB2 level and the analysis of failure mechanisms according to their thickness.

Based on the experimental results, the answer of the panel designed by the author may be compared to other already existing solutions, reported in the literature. Mention should be done for the mass ratio fabrics/panel of 0.709… 0.77 wt for all panels made by the author, which reflects an adequate laboratory-scale technology, with a high degree of repeatability and accuracy. The quality of the fabricated panels is also reflected in the standard deviation measured for the panels' thickness, which does not exceed 0.94 mm. Given the limited time and resources for this study, the research was conducted on sets of samples, for a specified number of layers (8 layers, 16 layers, 20 layers, 22 layers, 24 layers and 32 layers), in order to evaluate the quality of the panels for multiple hits (3 fires on each panel), the uniform response of the panels' set of the same thickness, and future research for using this type of panel (materials, technology) for a higher level of protection.

Behavior of panels at threats included in FB2 level and unfailed "material reserve" for 16- to 32-layer panels, based on SEM analysis, recommend the use of this technology for larger panels and testing them to threats of higher levels, especially FB3.

The author's contributions include:

- the realization, together with the specialists from the Research and Innovation Center for CBRN Defense and Ecology Bucharest, of a test campaign for the ballistic panels made by the author, in terms of the shutting equipment, measuring and monitoring devices,
- dissemination of results during the entire period of doctoral studies**,** starting with impact modeling and ending with experimental results,
- the composite recipe is original, based on materials with superior properties (quadriaxial fabric**s** **s**upplied by Castro Composite SL and Biresin CR82 resin supplied by Sika Company),
- laboratory-scale technology could be applied to produce high-strength composites and the parameters applied by the author have led to sets of protection panels with narrow standard deviations for panel thickness, surface density and, therefore, the mass ratio of fabrics panel,

- the test methodology had good results according to FB2 level, standard EN1522:2004 and EN1523:2004,
- analysis of the failure mechanisms of the materials involved in the impact with the help of macro photography, SEM images and EDX analysis.

6.4. Research Directions Open by This Thesis

In the field of ballistic protection equipment, everything is in a dynamic, spiral competition between penetrator and ballistic protection structure. The tendency of this competition is to obtain ballistic protection systems that are as flexible as possible and as resistant as possible to multiple hits and threats. The research directions in this field could be:

- obtaining and characterizing new composites and/or hybrid materials based on high strength fibers,
- ranking the obtained solutions based on criteria related to the flexibility of mobile equipment, specific density, maneuverability,
- simulation of impact phenomena and processes, at different levels, from micro to macro level, in order to make the most efficient use of material properties and their architectural particularities,
- expanding application of these ballistic protection solutions in civil industries, where there is a risk of impact (aerospace, energy industry, heavy industries, automotive industries, etc.).

The study carried out by the author may be continued in the following directions:

- design and testing of solutions for protective panels, hybrid or using materials lighter than those obtained only from glass fibers,
- design and testing of glass fiber panels, for applications other than ballistic, in particular for impact-resistant infrastructure, such as protection panels, made of high-performance fabrics,
- production and testing of protection panel products, made of high-performance fabrics, in compliance with the standards in force; this work has experimental results for 8-, 16- and 24-layer panels, but the realization and testing of intermediate panels as number of layers, between 10 layers and 16 layers, may lead to the reduction of the specific density, without affecting the safety in use,

- expanding the use of glass fiber fabrics, also in various combinations with other materials, in other domains where there is a risk of an impact (aeronautics, technological systems characterized by high values of working parameters, especially speed and load),
- the improvement of laboratory-scale technology in the sense of reducing resin losses and standardizing the tests,
- designing simulations with material models closer to their actual response, especially those depending on strain rate and temperature,
- designing a set of panels for higher levels of ballistic protection.

Author's
Scientific Work

Scientific papers published in journals indexes in ISI Thomson

1. Chiper Titire L., A. E. Musteata, A. Cioromila (Cantaragiu), G. C. Cristea, **Ojoc G. G.**, Deleanu L. (2021). Characterization of Blend PA6 +EPDM (60/40) by Tensile Tests. Materiale Plastice, 58(3), 51-63, WOS:000756838300001, https://doi.org/10.37358/MP.21.3.5503
2. Musteata, A. E., Petrescu, H., Cantaragiu Cioromila, A., **Ojoc, G. G.**, Deleanu, L. (2021). Influence of Composition on Energy at Break of Blends PP + PA6, *U.P.B. Scientific Buletin., Series B*, 83(3). WOS:000692192600012, https://www.scientificbulletin.upb.ro/rev_docs_arhiva/fulla95_317555.pdf
3. Pîrvu, C., Musteată, A.E.; **Ojoc G.G.**; Deleanu, L. (2020). Numerical and Experimental Results on Charpy Tests for Blends Polypropylene + Polyamide + Ethylene Propylene Diene Monomer (PP + PA + EPDM). Materials, 13, 5837. WOS:000602840500001, https://doi.org/10.3390/ma13245837
4. Pirvu C., Musteata A. E., **Ojoc G. G.**, Sandu S., Deleanu L. (2019). A meso level FE model for theimpact bullet – yarn. Materiale Plastice, 56(1), 22-31. WOS: 000464604100005, https://revmaterialeplastice.ro/pdf/5%20PARVU%201%2019.pdf

Scientific papers published in journals indexes in ISI proceedings

1. **Ojoc G. G.**, Pirvu C., Sandu S., Deleanu L., Glass fibers for impact protection systems. A review, the 8 th edition of International Conference on Material Science & Engineering, UgalMat 2018, October 11-13, 2018, Galati, Romania, https://iopscience.iop.org/article/10.1088/1757-899X/485/1/012019
2. **Ojoc G. G.**, Pirvu C., Sandu S., Deleanu L., Standardization in testing ballistic protection systems, RoTrib 2019, the 14th International Conference on Tribology, 19-21 September 2019, Cluj-Napoca, Romania, WOS:000619349400049, https://iopscience.iop.org/article/10.1088/1757-899X/724/1/012049

Scientific papers published in journals indexes in international data bases

1. Chiper L., **Ojoc G. G.**, Pirvu C., Deleanu L., Simulation of projectile impact on layered package made of unidirectional glass fibers, U.P.B. Sci. Bull., Series D, Vol. 83, Iss. 4, 2021, ISSN 1454-2358, pp. 253-266. https://www.scientificbulletin.upb.ro/rev_docs_arhiva/rezeb0_352712.pdf
2. **Ojoc G. G.**, Totolici Rusu V., Pîrvu C., Deleanu L., How Friction Could Influence the Shape and Failure Mechanism in Impact, With the Help of a Finite Element Model, U.P.B. Sci. Bull., Series D, Vol. 83, Iss. 3, 2021, ISSN 1454-2358, https://www.scientificbulletin.upb.ro/rev_docs_arhiva/reza6a_789278.pdf
3. **Ojoc G. G.**, Băbuț C., Ungureanu N., Deleanu L., FEM analysis of Storz coupling, Journal of Engineering Sciences and Innovation, 6(3), 2021, pp. 249–258, https://jesi.astr.ro/wp-content/uploads/2021/09/3_Ojoc-George-Ghiocel.pdf
4. **Ojoc G.-G.**, Rus V. T., Popescu C., Pirvu C., Deleanu L., Influence of friction in a case of impact simulation, INCAS Bulletin, Volume 12, Issue 4, 2020, pp. 145-154, DOI: 10.13111/2066-8201.2020.12.4.13; https://doi.org/10.13111/2066-8201.2020.12.4.13
5. **Ojoc G. G.**, Deleanu L., Georgescu C., Iorga D., Popescu M. V., Pîrvu C., Sandu S.,

Ballistic panel made of glass fiber fabrics + resin matrix for levels FB3 and FB5, Academia Forţelor Terestre „Nicolae Bălcescu" din Sibiu, Buletin ştiinţific supliment, Catalogul oficial al salonului „Cadet INOVA"® Nr. 5/2020, Cercetări şi inovaţii în viziunea tinerilor cercetători, pp. 336- 340, http://37.251.175.30/documente/Supliment_Inova_20.pdf

6. Totolici Rusu V., **Ojoc G. G.**, Pirvu C., Deleanu L., (2021). Influence of element size in a case of impact simulation. Mechanical Testing and Diagnosis, 10(4), 24-29. https://www.gup.ugal.ro/ugaljournals/index.php/mtd/article/view/4068

7. **Ojoc G.**, Oancea L., Pîrvu C., Sandu S., Deleanu, L. (2019). Modeling of impact on multiple layers with unidirectional yarns. Mechanical Testing and Diagnosis, 8(4), pp. 5-15. https://doi.org/10.35219/mtd.2018.4.01

8. **Ojoc G. G.**, Pirvu C., Sandu S., Deleanu L., Friction Modeling in Simulating Ballistic Impact. A Review, SERBIATRIB '19, 16th International Conference on, Tribology, Kragujevac, Serbia, 15 – 17 May 2019, http://pesjournal.net/journal/v1-n1/21.pdf

9. Guglea D., Ionescu T. F., Georgescu C., Dima D., **Ojoc G. G.**, Deleanu L., Boron Nitride as Additive in Rapeseed Oil, Tested on Four Ball Tester, SERBIATRIB '19, 16th International Conference on, Tribology, Kragujevac, Serbia, 15 – 17 May 2019, http://pesjournal.net/journal/v1-n1/76.pdf

10. Chiper L., **Ojoc G. G.**, Deleanu L., Pîrvu C. (2020). Simulation of impact behavior of a glass yarn. Mechanical Testing and Diagnosis, 10(1), 10-17, https://www.gup.ugal.ro/ugaljournals/index.php/mtd/article/view/4061

References[1]

[1] Abtew, M. A., Boussu F., Bruniaux, P, Loghin, C. & Cristian, I. (2019). Ballistic impact mechanisms – A review on textiles and fibre-reinforced composites impact responses. *Composites Structures,* 223(2), 110966, https://doi.org/10.1016/j.compstruct.2019.110966

[2] Agbossou, A., Cohen, I. & Muller, D. (1995) Effects of interphase and impact strain rates on tensile off-axis behavior of unidirectional glass fiber composite—Experimental results. *Engineering Fracture Mechanics,* 52(5) 923. https://doi.org/10.1016/0013-7944(94)00320-H

[3] Ahmad, S., Rasheed, A., Nawab, Y. (Editors) (2020). *Fibers for Technical Textiles*, Springer, Dordrecht, The Netherlands

[4] Alekseevskii, V. P. (1966). Penetration of a Rod into a Target at High Velocity, Combustion, Explosion and Shock Waves, 2, 63-66, Pleiades Publishing Ltd., Springer Verlag.

[5] Alil, L. C., Arrigoni, M., Deleanu L., & Istrate M. (2018). Assessment of delamination in Tensylon® UHMWPE composites by laser-induced shock. *Materiale plastice*, 55(3), 364-317. http://www.revmaterialeplastice.ro/pdf/24%20ALIL%20L%203%2018.pdf

[6] Alonso, L., Martínez-Herguetac, F., Garcia-Gonzalez, D., Navarro García-Castillo, C. S. K., & Teixeira-Dias, F. (2020). A finite element approach to model high-velocity impact on thin woven GFRP plates. *International Journal of Impact Engineering*. 142, 103593, https://doi.org/10.1016/j.ijimpeng.2020.103593.

[7] Anand, S. C. (2016). Technical fabric structures-knitted fabrics. In Horrocks A.R. & Anand S.C. (Eds.), *Handbook of Technical Textiles*. (2nd ed.) (pp. 107-162). Woodhead Publishing Ltd., Cambridge.

[8] Ansari, M. M., Chakrabarti, A. (2017). Impact behaviour of GFRP and Kevlar/epoxy sandwich compozite plate: Experimental and FE analyses, *Journal of Mechanical Science and Technology* 31(2), 771-776, doi 10.1007/s12206-017-0128-y

[9] Ashby, M. F. (2005). *Materials Selection in Mechanical Design*. Butterworth-Heinemann, Oxford, UK.

[10] Barre, S., Chotard, T., & Benzeggagh, M. L. (1996). Comparative study of strain rate effects on mechanical properties of glass fibre-reinforced thermoset matrix composites. *Composites Part A - Applied Science and Manufacturing.* **27**(12), 1169–1181.

[11] Bhatnagar, A. (2006). *Lightweight ballistic composites*. Woodhead Publishing Limited, CRC Press, Boca Raton, New York.

[12] Boccacinni, A. R. (2005). *Continuous fibre reinforced glass and glass-ceramic matrix composites*. Spinger.

[13] Børvik, T., Dey, S., & Clausen, A.H., (2009) Perforation resistance of five

[1] APA (7th edition), Common Reference Examples Guide, https://apastyle.apa.org/instructional-aids/reference-examples.pdf

different high-strength steel plates subjected to small-arms projectiles. International Journal of Impact Engineering. 36, 948-964. doi: 10.1016/j.ijimpeng.2008.12.003

[14] Cavallaro, P. V. (2011). Soft Body Armor: An overview of materials, manufacturing, testing, and ballistic impact dynamics, Naval Undersea Warfare Center Division Newport, Rhode Island, USA.

[15] Chang, A. L., Bodt B. E., (1977). JTCG/AS Interlaboratory Ballistic Test Program — Final Report, Army Research Laboratory - TR-1577 - December 1977, p. 12.

[16] Chen, X. W., Huang, X.L., Liang, G. J. (2011). Comparative analysis of perforation models of metallic plates by rigid sharp-nosed projectiles. *International Journal of Impact Engineering*, 38(7), 613-621. https://doi.org/10.1016/j.ijimpeng.2010.12.005

[17] Chowdhury, U., & Wu, X.-F. (2021). Cohesive zone modeling of the elastoplastic and failure behavior of polymer nanoclay composites. *Journal of Composites Science*, 5, 131. https://doi.org/10.3390/jcs5050131

[18] Ciobotaru, T. (2018). *Ingineria autovehiculelor militare cu șenile, Volumul I. Organizarea generală. Capacitatea de supraviețuir*e, Academia Tehnică Militară „Ferdinand I", București.

[19] Corona, E., & Reedlunn, B. (2013). A review of macroscopic ductile failure criteria. https://pdfs.semanticscholar.org/5404/27e7cd18762d80b311adc475825edf148a9b.pdf

[20] Cox, B. N., & Flanagan, G. (Editors) (1997). *Handbook of Analytical Methods for Textile Composites*, NASA Center for AeroSpace Information, USA.

[21] Cunniff, P. M. (1992). An analysis of the system effects in woven fabrics under ballistic impact. *Textile Research Journal*, 62, 9, 495-509, Report AD-A273 891. https://apps.dtic.mil/sti/pdfs/ADA273891.pdf

[22] Deleanu, L., Georgescu, C., Pîrvu, C., & Sandu, S. (2017). *Development of protection system,* Research contract 725/2017, "Dunarea de Jos" University of Galati, Romania

[23] Donea, J., Huerta A., Ponthot, J.-Ph., & Rodrıguez-Ferran A. (2004). Chapter 14. Arbitrary Lagrangian–Eulerian Methods. In Stein, E., de Borst R. & Hughes T. J. R. (Eds.), *Encyclopedia of Computational Mechanics*, Volume 1: Fundamentals. John Wiley & Sons, Ltd.

[24] Eichhorn, S. J., Hearle, J. W. S., Jaffe M., & Kikutani T. (Eds) (2009). *Handbook of textile fibre structure, Vol. 1: Fundamentals and manufactured polymer fibres*, Woodhead publishing limited.

[25] Fink, B. K. (October 2000). *Performance metrics for composite integral armor*. Technical Report ARL-RP- 8, U. S. Army Research Laboratory (ARL), Department of Chemistry, Oklahoma State University, Stillwater, USA. file:///C:/Users/Asus/Downloads/Performance_Metrics_for_Composite_Integr.pdf

[26] Giglio, M., Gilioli, A., Manes, A., Peroni L., & Scapin M. (2012). Investigation about the influence of the mechanical properties of lead. *EPJ Web of Conferences 26*, 04010. doi: 10.1051/epjconf/20122604010

[27] Grujicic, M., Pandurangan, B, Angstadt, D. C., Koudela, K. L., Cheeseman, B. A. (2007) Ballistic-performance optimization of a hybrid carbon-nanotube/E-glass reinforced poly-vinyl-ester-epoxy-matrix composite armor. *Journal of Materials Sci*ence. **42,** 5347–5359.

[28] Grujicic, M., Snipes, J., Ramaswami, S., Avuthu, V., (2016). Unit-cell-based derivation of the material models for armor-grade composites with different architectures of ultra-high molecular-weight polyethylene fibers. International Journal of Structural Integrity. 7(4), 458-489, doi: 10.1108/IJSI-06-2015-0015

[29] Hamouda, A. M. S., & Risby, M. S., 2006Modeling ballistic impact. In Bhatnagar A. (ed.), *Lightweight Ballistic Composites. Military and Law-Enforcement Applications* (pp. 101-126), Woodhead Publishing and Maney, CRC Press, Boca Raton, USA.

[30] Hancox, N. L. (2000). An overview of the impact behaviour of fibre reinforced composites, In Reid S. R., Zhou G. (Editors), *Impact behaviour of fibre-reinforced composite materials and structures* (pp. 1-32), CRC Press, Boca Raton, USA, Woodhead Publishing Limited, Cambridge, England.

[31] Horrocks, A. R., & Anand, S. C. (Editors) (2000). *Handbook of Technical Textiles*, Woodhead Publishing Limited and The Textile Institute, Cambridge, England.

[32] Hosford, W. F. (2010). *Mechanical Behavior of Materials*, (2nd ed.), Cambridge University Press, UK.

[33] Ingle, S., Yerramalli, C. S., Guh,a A., & Mishra, S. (2021). Effect of material properties on ballistic energy absorption of woven fabrics subjected to different levels of inter-yarn friction. *Composite Structures*, 266, 113824. doi: 10.1016/j.compstruct.2021.113824

[34] Ionescu, T. F., Pîrvu C., Badea, S, Georgescu, C., & Deleanu, L. (2017). The influence of friction characteristics in simulating the impact bullet − stratified materials. *15th International Conference on Tribology, SerbiaTrib'17,* Kragujevac, Serbia.

[35] Johnson, G. R., & Cook, W. H. (1985). Fracture characteristics of three metals subjected to various strains, strain rates, temperatures and pressures. *Engineering Fracture Mechanics*, 21, 31-48.

[36] Joki, R. K., Grytten, F., Hayman, B., & Sørensen, B. F. (2016). Determination of a cohesive law for delamination modelling - Accounting for variation in crack opening and stress state across the test specimen width. *Composites Science and Technology*, 128, 49-57. 10.1016/j.compscitech.2016.01.026

[37] Kneubuehl, B. P. (2003). Ballistic protection, Hun, Switzerland, English edition, http://www.vpam.eu/fileadmin/Wissenswertes/Ballistic-protection.pdf

[38] Laible, R. C. (ed.), (1980). *Ballistic Materials and Penetration Mechanics*, Elsevier Scientific Publishing Company, Amsterdam, The Netherlands.

[39] Lee, B. L., Walsh, T. F., Won, S. T., Patts, H. M., Song, J. W., & Mayer, A. H. (2001). Penetration failure mechanisms of armor-grade fiber composites under impact. *Journal of Composite Materials*, 35(18), 1605-1633.

[40] Lee, H.-H., (2021). *Finite Element Simulations with ANSYS Workbench 2021*. SDC Publications. USA.

[41] Lombard, D. B. (1961). *The Hugoniot Equation of State of Rocks*, United States, Web.

[42] Lowenstein, K. L. (1993). *The manufacturing technology of continuous glass fibres* (3rd ed.), Springer, Amsterdam, the Netherlands.

[43] Ma, D., Manes, A., Campos Amico, S., Giglio, M. (2019). Ballistic strain-rate-dependent material modelling of glass-fibre woven composite based on the prediction of a meso-heterogeneous approach. *Composite Structures*, 216, 187–200.

[44] Ma, X., Zhang, Q., & Zhang, X. (2022). A model for rigid asymmetric ellipsoidal projectiles penetrating into metal plates, *International Journal of Impact Engineering*. 163, 104140. https://doi.org/10.1016/j.ijimpeng.2021.104140.

[45] Mallick, P. K. (2007). *Fiber Reinforced Composites Materials, Manufacturing and Design*. (2nd ed.) (pp. 60-116), CRC Press, Florida, USA.

[46] Meyer, C. S., O'Brien, D. J., (Gama) Haque, B. Z., Gillespie, Jr. J. W. (2022). Mesoscale modeling of ballistic impact experiments on a single layer of plain weave composite. *Composites Part B*, 235, 109753. https://doi.org/10.1016/j.compositesb.2022.109753

[47] Meyers, M. A. (1994). *Dynamic Behavior of Materials*. John Wiley & Sons, Inc., USA.

[48] Múgica, J. I., Aretxabaleta, L., Ulacia, I., & Aurrekoetxea, J. (2016). Rate-dependent phenomenological model for self-reinforced polymers. *Composites: Part A*, 84, 96-102.

[49] Naik, N. (2004). Composite structures under ballistic impact. *Composite Structures,* 66(1-4), 579-590.

[50] Naresh, K., Shankar, K., Rao, B. S., & Velmurugan, R. (2016). Effect of high strain rate on glass/carbon/hybrid fiber reinforced epoxy laminated composites. *Composites Part B*, 100, 125-135. http://dx.doi.org/10.1016/j.compositesb.2016.06.007

[51] Nilakantan, G, & Nutt, S. (2017). Effects of ply orientation and material on the ballistic impact behavior of multilayer plain-weave aramid fabric targets, *Defence Technology,* 1-14.

[52] Ojoc, G. G., Oancea, L., Pîrvu, C., Sandu, S., & Deleanu, L. (2019). Modeling of impact on multiple layers with unidirectional yarns. *Mechanical Testing and Diagnosis*, 8(4), 5-15, https://doi.org/10.35219/mtd.2018.4.01

[53] Ojoc, G. G., Pîrvu, C., Sandu, S., & Deleanu, L. (2019, 19-21 September). Standardization in testing ballistic protection systems, RoTrib 2019, the 14th International Conference on Tribology, Cluj-Napoca, Romania.

[54] Park, R, & Jang, J. (1998). A study of the impact properties of compozites consisting of surface-modified glass fibers in vinyl ester resin. *Composites Science and Technology,* 58(6) 979-985.

[55] Peroni, L., Scapin, M., Fichera, C., Manes A., & Giglio, M. (2012). Mechanical properties at high strain-rate of lead core and brass jacket of a NATO 7.62 mm ball bullet in numerical simulations of ballistic impacts. in Proceedings of *DYMAT 2012.*

[56] Potluri, R., Supriya, K., & Vittal, G. V. G. (2018). Effect of boron carbide particles inclusion on the mechanical behaviour of S2-Glass fiber based polyester composites. *Material Today. Proceedings.* 5(9/3), 20257-20267. https://doi.org/10.1016/j.matpr.2018.06.397

[57] Rebouillat, S., Steffenino, B., & Miret-Casas, A. (2010). Aramid, steel, and glass: characterization via cut performance testing, of composite knitted fabrics and their constituent yarns, with a review of the art, *Journal of Materials Science*, 45, 5378–5392, doi: 10.1007/s10853-010-4590-5

[58] Sabet, A., Fagih, N., & Beheshty, M. B. (2011). Effect of reinforcement type on high velocity impact response of GRP plates using a sharp tip projectile. *International Journal of Impact Engineering,* 38, 715-722.

[59] Safta, I. (2011). *Contribuţii la studiul teoretic şi experimental al mijloacelor individuale de protecţie balistică.* teză de doctorat, Academia Tehnică Militară „Ferdinand I", Bucureşti, 2011.

[60] Sathishkumar, T. P., Satheeshkumar, S., & Naveen, J. (2014). Glass fiber-reinforced polymer composites – a review, *Journal of Reinforced Plastics and Composites*, 33(13), 1258–1275.

[61] Schwer, L. (2007) Optional Strain-Rate Forms for the Johnson Cook constitutive model and the role of the parameter Epsilon_01, Dynamore GmbH, LS-Dyna, Andwerderforum, Frankenthal, Impact, https://www.dynamore.de/en/downloads/papers/07-forum/impact/optional-strain-rate-forms-for-the-johnson-cook/view

[62] Sockalingam, S. (2016). *Transverse Impact of Ballistic Fibers and Yarns – Fiber Length-Scale Finite Element Modeling and Experiments*, PhD thesis, University of Delaware, USA. http://udspace.udel.edu/handle/19716/19972

[63] Tanoglu, M., McKnight, S., Palmese, G., & Gillespie, Jr J. (2001). The effects of glass-fiber sizings on the strength and energy absorpentruion of the fiber/matrix interphase under high loading rates, *Composites Science and Technology,* 61(2), pp. 205-220.

[64] Wallenberger, F.T., Watson, J. C., & Li, H. (2001). *Glass Fibers. ASM Handbook. 21: Composites* (pp. 27-34). American Technical Publishers Ltd., Ohio, USA.

[65] Walters, W., Williams, C., & Normanidia M., (2006). An Explicit Solution of the Alekseevskii-Tate Penetration Equations, *International Journal of Impact Engineering*, 33, 837-846.

[66] Wiśniewski, A. & Gmitrzuk, M. (2013). Validation of numerical model of the Twaron CT709 ballistic fabric. Proceedings of *27th International Symposium on Ballistics, BALLISTICS 2013*, 2, 1535-1544.
[67] Xanthos, M. (2010). *Functional Fillers for Plastics* (2nd edition) (pp. 1.1-1.18), Wiley-VCH Verlag GmbH & Co. KGaA, Weinheim
[68] Zhu, F. (2009). *Advanced Materials for Composite Armour*, PhD thesis, School of Engineering and Materials, „Queen Mary" University of London, UK.
[69] *** 2011 *Opportunities in protection materials science and technology for future army applications*, Committee on Opportunities in Protection Materials Science and Technology for Future Army Applications National Research Council, ISBN 978-0-309-21285-4
[70] *** 4.12. Cohesive Zone Material (CZM) Model, Release 18.2 - © ANSYS, Inc.
https://www.mm.bme.hu/~gyebro/files/ans_help_v182/ans_thry/thy_mat11.html
[71] *** ANSYS Explicit Dynamics Analysis Guide (2021). ANSYS, Inc., USA
[72] *** Ballistic Materials Handbook, Aramids by Teijin, QMB1.1 20181001EN, 2020
[73] *** Ballistic (accesat 11.02.2022).
https://www.protectolite.com/ballistic/industries.html,
[74] *** Biresin® CR82.Composite resin system, (accesat 4.10.2020).
https://industry.sika.com/dms/getdocument.get/93a3a9b1-7291-47ce-8ca7-18ae3f458043/Biresin-CR82-New.pdf
[75] *** Noi soluții de blindaje, proiect Protectcomb,
https://www.rumaniamilitary.ro/noi-solutii-de-blindaje-ieftine-si-la-indemana (accesat 24.03.2022)
[76] *** CEN CENELEC Declaration, Standards build trust, (accesat 20.7.2021).
https://www.cencenelec.eu/news/publications/Publications/CENCENELEC-DECLARATION-Final.pdf
[77] *** EN 1522:2004 Windows, doors, shutters and blinds. Bullet resistance. Requirements and classification
[78] *** EN 1523:2004 Windows, doors, shutters and blinds - Bullet resistance - Test method
[79] *** Glass (accesat 3.02.20210).
https://www.castrocompositesshop.com/en/63-glass, (accesat 22.02.2022)
[80] *** 1200 g/m2 Quadriaxial Stitched Glass Fabric (0º/+45º/90º/-45º), 127 cm wide (accesat 12.01.2022). https://www.castrocompositesshop.com/en/fibre-reinforcements/1204-1200-gm2-quadriaxial-stitched-glass-fabric-0%C2%BA45%C2%BA90%C2%BA-45%C2%BA-127-cm-wide.html
[81] *** NIJ 0108 ± ballistic resistant protective materials National Institute of Justice,
[82] ***Sika Group. About us (accesat 3.10.2021),
https://www.sika.com/en/home.html